
COLA: COLLABORATIVE ADAPTATION WITH GRADIENT LEARNING

Enmao Diao

Department of Electrical and Computer Engineering
Duke University
enmao.diao@duke.edu

Qi Le

Department of Computer Science and Engineering
University of Minnesota-Twin Cities
le000288@umn.edu

Suya Wu

Department of Electrical and Computer Engineering
Duke University
suya.wu@duke.edu

Xinran Wang

Department of Computer Science and Engineering
University of Minnesota-Twin Cities
wang8740@umn.edu

Ali Anwar

Department of Computer Science and Engineering
University of Minnesota-Twin Cities
aanwar@umn.edu

Jie Ding

School of Statistics
University of Minnesota-Twin Cities
dingj@umn.edu

Vahid Tarokh

Department of Electrical and Computer Engineering
Duke University
vahid.tarokh@duke.edu

ABSTRACT

A primary function of back-propagation is to compute both the gradient of hidden representations and parameters for optimization with gradient descent. Training large models requires high computational costs due to their vast parameter sizes. While Parameter-Efficient Fine-Tuning (PEFT) methods aim to train smaller auxiliary models to save computational space, they still present computational overheads, especially in Fine-Tuning as a Service (FTaaS) for numerous users. We introduce Collaborative Adaptation (CoLA) with Gradient Learning (GL), a parameter-free, model-agnostic fine-tuning approach that decouples the computation of the gradient of hidden representations and parameters. In comparison to PEFT methods, CoLA facilitates more cost-effective FTaaS by offloading the computation of the gradient to low-cost devices. We also provide a theoretical analysis of CoLA and experimentally demonstrate that CoLA can perform on par or better than existing PEFT methods on various benchmarks. Our code is available [here](#).

1 INTRODUCTION

Transfer learning with pretrained foundation models plays a crucial role in deep learning applications such as natural language processing and computer vision. Adapting these models to specific tasks via fine-tuning has become a prevalent paradigm (Peters et al., 2018; Fedus et al., 2022; Devlin et al., 2018). However, full Fine-Tuning (FT), which modifies all model parameters, becomes computationally prohibitive because each data task requires a unique set of fine-tuned parameters. The size of recent deep models has dramatically increased, ranging from hundreds of millions (Radford et al., 2019; Lewis et al., 2019) to hundreds of billions (Brown et al., 2020; Muennighoff et al., 2022) or even trillions (Fedus et al., 2022) of parameters. As these models continue to expand, developing efficient methods for adaptation and deployment becomes imperative. In response to these challenges, Parameter-Efficient Fine-Tuning (PEFT) has been introduced (Houlsby et al., 2019; Zaken et al., 2021; Li & Liang, 2021; Hu et al., 2021; He et al., 2021). Specifically, PEFT methods

update only a small number of free parameters, with the amount less than 1% of the original model parameters, while keeping the pretrained parameters frozen. These methods can achieve comparable performance to full FT on various tasks and significantly reduce the computational cost (Hu et al., 2021; He et al., 2021).

In an era where personalized models are increasingly in demand, we aim to develop a system to provide Fine-Tuning as a Service (FTaaS) for numerous users. However, existing PEFT methods introduce significant computational overhead because each user would require a separate set of trainable parameters and their corresponding gradient for fine-tuning with gradient descent (Dettmers et al., 2023). Due to the constraints of computational space in edge devices, handling these extra parameters becomes challenging, especially when offering FTaaS to a large number of users. In this work, we introduce Collaborative Adaptation (CoLA) with Gradient Learning (GL), a parameter-free and model-agnostic fine-tuning method that decouples the computation of the gradient of hidden representations and parameters. Our proposed method offers a more cost-efficient FTaaS system compared with PEFT methods, enhancing collaboration between the central server and local users. This efficiency improvement is achieved by offloading the computation of the parameter gradient to lower-cost devices, thereby conserving computational resources.

Our contributions are threefold:

- We introduce Gradient Learning (GL), a new learning framework based on functional gradient descent, specifically designed to decouple the computation of the gradient of hidden representations and parameters. A theoretical analysis of GL is provided, showcasing its equivalence to the classical gradient descent method.
- We conceptualize Fine-Tuning as a Service (FTaaS) and propose Collaborative Adaptation (CoLA) with GL as a cost-effective solution for FTaaS by offloading the computation of the gradient to low-cost devices. We utilize the parameter merging technique to further reduce the cost of computation space and to integrate multiple adapters for collaboratively leveraging local computation resources.
- Through comprehensive experiments on diverse benchmarks, we demonstrate that CoLA consistently matches or outperforms existing PEFT methods in performance. We conduct a comprehensive quantitative evaluation of computational costs on real devices. We also provide a theoretical analysis of parameter merging, present empirical results underscoring the benefits of user collaboration, and conduct ablation studies.

2 RELATED WORKS

Parameter-Efficient Fine-Tuning (PEFT) PEFT methods aim to fine-tune large pretrained models to downstream tasks. To achieve computational efficiency, they freeze the parameters of the pretrained network while fine-tuning a small set of tunable parameters. Previous works propose to insert Adapter layers between existing layers in the pretrained network (Rebuffi et al., 2017; Housby et al., 2019). However, this sequential nature can lead to inference latency, particularly with small batch sizes, as the Adapter layers have to be processed sequentially and the extra computation cannot be bypassed directly (Hu et al., 2021). In contrast, Prefix Tuning (Li & Liang, 2021) and Low-Rank Adaptation (LoRA) (Hu et al., 2021) offer parallel computations for inference. Prefix Tuning prepends a sequence of continuous vectors, referred to as the “prefix”, to the input or hidden layers. This prefix can be seen as the tunable instruction prompting applied to the word embeddings. Nevertheless, it has been noted that Prefix Tuning suffers from optimization difficulty and lack of stability (Li & Liang, 2021; Hu et al., 2021). LoRA (Hu et al., 2021) introduces two trainable low-rank matrices to reparameterize the updates of pretrained weight matrices in downstream tasks. This approach avoids additional inference computation by merging the fine-tuned matrices together with the frozen pretrained weights. A unified framework of PEFT including Adapter (Housby et al., 2019), Prefix Tuning (Li & Liang, 2021), and LoRA (Hu et al., 2021) has been proposed by He et al. (2021). Specifically, it shows an alternative form of Prefix Tuning, revealing its close relationship with Adapter tuning, and then it conceptualizes PEFT as the process of learning a modification of hidden representations. Recent advances such as few-shot (Liu et al., 2022) and quantized (Dettmers et al., 2023) fine-tuning methods are proposed to further enhance the computational efficiency. Existing PEFT methods primarily focus on *modeling* various additional tunable structures to reduce computational cost on fine-tuning. In contrast, we propose a computationally efficient *learning* al-

gorithm for fine-tuning large models for downstream tasks, which is, to our best knowledge, the first work on this focus.

Functional gradient descent Functional gradient descent generalizes gradient descent by optimizing a loss function within a function space rather than a parameter space. Mason et al. (1999) introduces an alternative view of boosting algorithms as iterative functional gradient descent algorithms, which has led to the recent advanced development of Gradient Boosting (GB) (Friedman, 2001) in the area of deep learning (Nitanda & Suzuki, 2018; Huang et al., 2018; Diao et al., 2022). TrAdaBoost (Dai et al., 2007) extends AdaBoost (Freund & Schapire, 1995) to transfer learning with classical machine learning models. It utilizes the boosting algorithm to learn a new classifier to adapt changes in the training data. Our work is primarily inspired by Gradient Assisted Learning (GAL) (Diao et al., 2022), which uses GB within a decentralized collaborative learning framework. It promotes collaboration in supervised learning without sharing local data, models, or objective functions. Existing functional gradient descent methods like GB and GAL train a *distinct* model for each *non-stochastic* boosting iteration, utilizing the “pseudo-residual” that approximates the gradient of the model’s *output*. In contrast, our proposed method fine-tunes the *same* model at each *stochastic* boosting iteration using the gradient of *hidden representations*, so that an ensemble of weak learners is no longer needed. Furthermore, we concurrently apply stochastic functional gradient descent in multiple intermediate layers of pretrained large models and extend our algorithm to a distributed setting to promote collaboration among local users.

3 METHOD

3.1 PROBLEM

Fine-Tuning (FT) Consider a dataset of N samples, denoted by $\mathcal{D} = \{(x_i, y_i)\}_{i=1}^N$, where x_i is the input and y_i is the corresponding target. Suppose the architecture of a deep neural network $f_\theta(\cdot)$ contains M distinct layers, each represented by $f_{\theta_m}(\cdot)$ for $m = 1, \dots, M$. For each layer m , the network processes a specific hidden input $x_{i,m}$ and consequently produces a hidden representation, denoted by $h_{i,m} = f_{\theta_m}(x_{i,m})$. In subsequent notations, we omit the index i for clarity. Note that the hidden input x_m for any layer m refers to the hidden representation of its preceding layer. In the special case of the first layer, $x_{i,1}$ corresponds to the input data x_i of dataset \mathcal{D} . Given a pretrained network $f_{\theta_{1:M}}(\cdot)$, the objective is to minimize its empirical risk in order to fine-tune the model, which can be represented by

$$\min_{\theta_{1:M}} \mathbb{E}_N \mathcal{L}(y, f_{\theta_{1:M}}(x)), \quad (1)$$

where $\mathcal{L}(\cdot)$ is the loss function and \mathbb{E}_N denotes the empirical average over the dataset \mathcal{D} . A conventional fine-tuning method utilizes gradient descent for parameter optimization by computing the derivative of the loss with respect to the model parameters $\theta_{1:M}$, written as

$$\nabla \theta_{1:M} \triangleq \nabla_{\theta_{1:M}} \mathbb{E}_N \mathcal{L}(y, f_{\theta_{1:M}}(x)). \quad (2)$$

Parameter-Efficient Fine-Tuning (PEFT) Parameter-Efficient Fine-Tuning (PEFT) has been introduced to reduce the computational cost of fine-tuning large models such as Large Language Models (LLM). PEFT methods typically incorporate an auxiliary model, denoted as $g_{w_m}(\cdot)$, which is parameterized by w_m for each layer m . During the fine-tuning process, PEFT methods freeze the original model parameters $\theta_{1:M}$ and only update the auxiliary parameters $w_{1:M}$. A notable advantage of this approach is that the dimensionality of $w_{1:M}$ tends to be considerably smaller than that of $\theta_{1:M}$, leading to substantial savings in storage requirements of back-propagation, especially in the memory usage of Graphics Processing Units (GPU). Low-Rank Adaptation (LoRA), one of the most widely used PEFT methods, ingests the hidden input $x_{i,m}$ and produces a change of hidden representation $\Delta h_{i,m}$. The fine-tuned hidden representation $\hat{h}_{i,m}$ will be used in the original network as a fine-tuned replacement of h_m as described by

$$\Delta h_{i,m} = g_{w_m}(x_{i,m}), \quad \hat{h}_{i,m} = h_{i,m} + \alpha \cdot \Delta h_{i,m},$$

where α is a scaling factor that can be tuned during inference. The fine-tuned model is denoted by $f_\theta(x, \Delta h_{1:M})$. Given a pretrained network $f_{\theta_m}(\cdot)$, the objective of LoRA becomes $\min_{w_{1:M}} \mathbb{E}_N \mathcal{L}(y, f_\theta(x, \Delta h_{1:M}))$, and it can be optimized by computing the derivative of the loss with respect to the auxiliary parameters $w_{1:M}$ as follows

$$\nabla w_{1:M} \triangleq \nabla_{w_{1:M}} \mathbb{E}_N \mathcal{L}(y, f_\theta(x, \Delta h_{1:M})). \quad (3)$$

3.2 COLLABORATIVE ADAPTATION

We propose Collaborative Adaption (CoLA) as a framework for providing Fine-Tuning as a Service (FTaaS) with our novel Gradient Learning (GL) algorithm. GL is both *parameter-free* and *model-agnostic* because it decouples the computation of the gradient of auxiliary parameters from that of the fine-tuned hidden representations, a process we refer to as *Gradient Decoupling*. Meanwhile, our method can significantly improve computational efficiency and provide cost-effective service for many users by offloading the computation of the gradient to low-cost devices.

Gradient Learning (GL) We propose Gradient Learning (GL) in order to save the storage requirements of back-propagation. Existing PEFT methods focus on optimizing the parameter efficiency of the auxiliary model $g_{w_m}(\cdot)$ to achieve the same goal. Specifically, PEFT methods fine-tune the pretrained model for downstream tasks by leveraging a set of auxiliary parameters, denoted as $w_{1:M}$, while keeping the original parameters $\theta_{1:M}$ frozen. Unlike full FT, this strategy bypasses the computation of $\nabla\theta_{1:M}$ during the back-propagation phase. Efficiency is further enhanced by minimizing the size of these auxiliary parameters. Without explicitly optimizing $\theta_{1:M}$, it has been shown that optimizing $w_{1:M}$ can still achieve satisfactory results (Hu et al., 2021; He et al., 2021). In order to optimize the auxiliary parameters $w_{1:M}$, the back-propagation procedure of PEFT methods computes $\nabla w_{1:M}$, and consequently, the gradient of fine-tuned hidden representations through chain rule, denoted as

$$\nabla\hat{h}_{1:M} \triangleq \nabla_{\hat{h}_{1:M}} \mathbb{E}_N \mathcal{L}(y, f_{\theta}(x, \Delta h_{1:M})). \quad (4)$$

On the contrary, GL is a new learning algorithm that decouples the computation of the gradient of auxiliary parameters $\nabla w_{1:M}$ and fine-tuned hidden representations $\nabla\hat{h}_{1:M}$. At the beginning, we forward data x and the change of hidden representations $\Delta h_{1:M}$ into both the pretrained base model and the newly initialized auxiliary models to obtain the model output $f_{\theta}(x, \Delta h_{1:M})$ and fine-tuned hidden representations $\hat{h}_{1:M}$. Then, we compute the gradient of fine-tuned hidden representations $\nabla\hat{h}_{1:M}$ which naturally exist in the back-propagation stage of deep neural networks. Meanwhile, if $\alpha = 1$ and using $\frac{\partial\hat{h}_{1:M}}{\partial\Delta h_{1:M}} = \alpha$, we have the gradient of fine-tuned hidden representations equal to the gradient of the change of hidden representation as follows

$$\nabla\hat{h}_{1:M} = \nabla_{\Delta h_{1:M}} \mathbb{E}_N \mathcal{L}(y, f_{\theta}(x, \Delta h_{1:M})). \quad (5)$$

It is essential to note that during the back-propagation stage, GL does not compute the gradient of either the original or the auxiliary parameters. After completing the forward and backward propagation stages, we can transfer the hidden inputs $x_{1:M}$ and the gradient of the fine-tuned hidden representations $\nabla\hat{h}_{1:M}$ to multiple low-cost devices, such as Central Processing Unit (CPU) or low-end GPUs. By doing so, we reduce the cost of computational space on resource-intensive devices which host the large base model. We refer to this process as *Gradient Offloading*. Our proposed approach offers a significant computational advantage, because the computational space of the GPU hosting the large base model is considerably more valuable than that of low-end GPUs, CPUs and storage drives. Furthermore, computing the gradient of auxiliary parameters on low-cost devices will not disrupt the computation of the gradient of hidden representations on the GPU, where the large base model is hosted. As a result, we can run two decoupled gradient computations in parallel for different batches of data.

Next, we can optimize the auxiliary models $x_{1:M} \mapsto g_{w_{1:M}}(x_{1:M})$ in parallel on multiple low-cost device. We achieve this by fitting the target $\Delta h_m - \nabla\hat{h}_m$, which are calculated from the last update and treated as a fixed term. For instance, we define the auxiliary quadratic loss as follows

$$\begin{aligned} \ell_m(x, y; w_m) &\triangleq \frac{1}{2} \|g_{w_m}(x_m) - (\Delta h_m^t - \nabla\hat{h}_m^t)\|_2^2, \text{ where} \\ \Delta h_m^t &\triangleq g_{w_m^t}(x_m), \quad \nabla\hat{h}_m^t \triangleq \left. \frac{\partial\mathcal{L}(y, f_{\theta}(x, \Delta h_{1:M}^t))}{\partial\hat{h}_m} \right|_{\hat{h}_m = h_m + \Delta h_m^t} \end{aligned} \quad (6)$$

and w_m^t represents the most recent estimate of w_m at round t . We then operate gradient-based optimizations using (6). Its validity is justified by the following result.

Proposition 1 The gradient $\nabla_{w_m} \ell_m(x, y; w_m)$ and $\nabla_{w_m} \mathcal{L}(y, f_\theta(x, \Delta h_{1:M}))$ evaluated at $w_m = w_m^t$ are the same for any w_m^t .

The gradient of the updated auxiliary model $g_{w_m}(\cdot)$ essentially moves w_m toward the optimal direction of h_m that minimizes the objective loss. Intuitively, we reconstruct the computation graph of the auxiliary model $g_{w_m}(\cdot)$ with the hidden input x_m and optimize the auxiliary parameters w_m with the change of hidden representations Δh_m and the gradient of fine-tuned representations $\nabla \hat{h}_m$. It is essential to note that the optimization of $g_{w_m}(\cdot)$ is decoupled from the computation of $\nabla \hat{h}_{1:M}$. In practice, we can optimize $g_{w_{1:M}}(\cdot)$ by taking one step of gradient descent with a learning rate γ on multiple low-cost devices in parallel without interfering with the computation of $\nabla \hat{h}_{1:M}$ on the high-cost GPU hosting the large base model.

Existing learning algorithms compute the gradient of hidden representations and parameters concurrently during back-propagation. However, this classical approach is significantly limited by the computation space of the high-cost device, which further restricts the training batch size, thus affecting the overall training time of deep neural networks. Our approach demonstrates that we can train the network by computing the gradient of hidden representations and parameters separately. Additionally, storage limitations also affect the choice of auxiliary models, impacting fine-tuning performance. Our method allows for a broader selection of auxiliary models, as their optimization can be done on a different device. Theoretically, our proposed Gradient Learning (GL) is related to functional gradient descent and Gradient Boosting (GB) (Friedman, 2001). Our work is primarily inspired by Gradient Assisted Learning (GAL), a recent advance of functional gradient descent in distributed machine learning (Diao et al., 2022). While methods like GB and GAL use a unique model for every non-stochastic boosting iteration at the output layer, our GL method retrains the same model for every stochastic boosting iteration at intermediate layers.

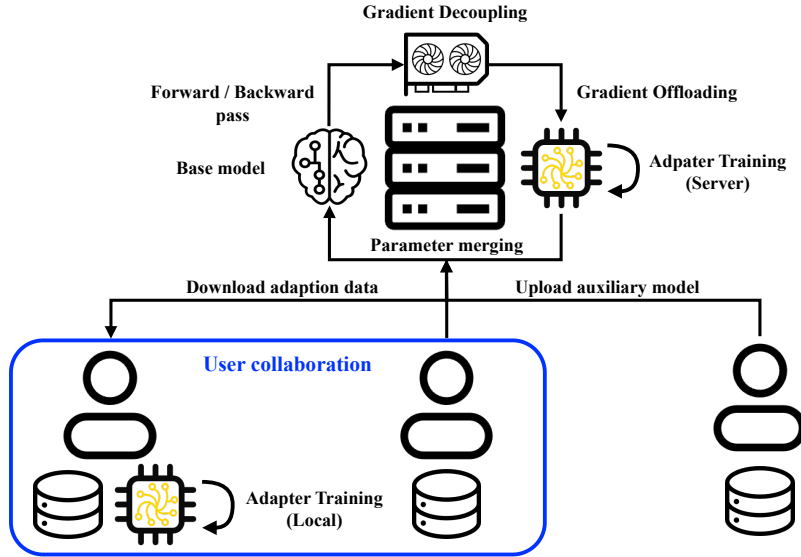


Figure 1: Illustration of the Fine-Tuning as a Service (FTaaS) system architecture. A central server handles both forward and backward passes of the pretrained model. It offloads gradient computations to a low-cost device, namely, *Gradient Offloading*. Meanwhile, adapters can be trained either on the server or locally by downloading adaptation data. Users of FTaaS can train their adapters independently or collaborate with others if needed.

Fine-Tuning as a Service (FTaaS) As illustrated in Figure 1, we propose a computationally scalable approach for Fine-Tuning as a Service (FTaaS) designed to prevent the cost of computational space on the GPU from increasing proportionally with the number of users of the service. Notably, given the constraints of computational space when fine-tuning large models on GPU, we introduce Collaborative Adaptation (CoA) with GL through a stochastic optimization procedure as detailed in Algorithm 1. During each training iteration t , a batch of data from K users $(x_{1:K}^t, y_{1:K}^t)$ of size B is sampled from the training dataset $(x_{1:K}, y_{1:K})$. At $t = 1$, the auxiliary parameters $w_{1:M,1:K}$ are initialized to zero. After receiving $M \times K$ auxiliary models from K collaborative users, we can

compute the output of the model $f_\theta(x_{1:M,1:K}^t, \Delta h_{1:M,1:K}^t)$, where $\Delta h_{m,k}^t \triangleq g_{m,k}^t(x_{m,k}^t)$. Then, we gather the hidden input of auxiliary models $x_{1:M}^t$ during the forward pass, achievable via the `hook` functionality in Pytorch (Paszke et al., 2019). Next, we compute the backward pass of the loss $\mathcal{L}(y_{1:K}^t, f_\theta(x_{1:M,1:K}^t, \Delta h_{1:M,1:K}^t))$ on GPU, transfer and save the hidden input of auxiliary models $x_{1:M,1:K}^t$ and the gradient of fine-tuned hidden representations $\nabla \hat{h}_{1:M,1:K}^t$ to buffers on low-cost devices. Due to the computational space constraints of batch size B on the GPU, we use buffers to accumulate adequate adaptation data over I batches, where I is referred to as the adaptation interval in Algorithm 1. By increasing I , we can effectively increase the batch size, which may allow for faster model convergence due to a more accurate estimate of the gradient of the auxiliary parameters. Once the buffers collect sufficient adaptation data, we can optimize each auxiliary model $g_{w_{m,k}}^t$ in parallel following Equation 6. Similar to ZeRO-Offload (Ren et al., 2021), our method can also save the state information of adaptive optimizers like AdamW on low-cost devices. Notably, each training iteration only involves one forward and backward pass on GPU, which is the same as the classical gradient descent procedure. The distinction is that we decouple and offload the computation of the gradient of parameters to separate devices.

Algorithm 1 CoLA: Collaborative Adaptation with Gradient Learning

Require: Training data set x and target y , a base model $f_\theta(\cdot)$, M fine-tuning layers, K collaborative users, $M \times K$ auxiliary models $g_{w_{1:M,1:K}}(\cdot)$, the number of training iterations T , the loss function \mathcal{L} , the training batch size B , the learning rate γ , and the adaptation interval I .

- 1: **for** each training iteration t from 1 to T **do**
 - 2: $(x_{1:K}^t, y_{1:K}^t) \leftarrow$ Sample a batch of size B from the training dataset $(x_{1:K}, y_{1:K})$
 - 3: (Optional) Merge $M \times K$ auxiliary models of K users to the base model
 - 4: Compute forward pass of $f_\theta(x_{1:M,1:K}^t, \Delta h_{1:M,1:K}^t)$, with $\Delta h_{m,k}^t \leftarrow g_{m,k}^t(x_{m,k}^t)$
 - 5: Gather hidden input of auxiliary models $x_{1:M,1:K}^t$ from forward pass
 - 6: Compute backward pass of $\mathcal{L}(y_{1:K}^t, f_\theta(x_{1:M,1:K}^t, \Delta h_{1:M,1:K}^t))$
 - 7: Gather gradient of hidden representations
 $\nabla \hat{h}_{1:M,1:K}^t = \nabla_{\hat{h}_{1:M,1:K}^t} \mathcal{L}(y_{1:K}^t, f_\theta(x_{1:M,1:K}^t, \Delta h_{1:M,1:K}^t))$
 - 8: (Optional) Unmerge $M \times K$ auxiliary models of K users from the base model
 - 9: Transfer $(x_{1:M,1:K}^t, \nabla \hat{h}_{1:M,1:K}^t)$ to low-cost devices
 - 10: **for** each adapter m of user k *in parallel* **do**
 - 11: Save adaptation data $(x_{m,k}^t, \nabla \hat{h}_{m,k}^t)$ to buffer
 - 12: **if** $t \bmod I = 0$ **then**
 - 13: Compute forward pass $\Delta h_{m,k}^{t-I:t} = g_{w_{m,k}}^t(x_{m,k}^{t-I:t})$
 - 14: Optimize $g_{w_{m,k}}^t(\cdot)$ with $(x_{m,k}^{t-I:t}, \Delta h_{m,k}^{t-I:t} - \nabla \hat{h}_{m,k}^{t-I:t})$ and learning rate γ^t
 - 15: Transfer auxiliary model $g_{w_{m,k}}^t(\cdot)$ to the server
 - 16: Empty buffer
-

Parameter merging We study and integrate parameter merging into our algorithm to further reduce the cost of computation space. Previous work has demonstrated that the original parameters θ_m and the auxiliary parameters w_m can be merged into one network after fine-tuning is finished for inference (He et al., 2021; Mangrulkar et al., 2022). PEFT methods like LoRA offer such capability, and its tuning factor α can adjust the contribution of the adapter to the output of the model. Additionally, this approach can also combine multiple adapters trained on different datasets. We propose to optionally utilize parameter merging during training, as shown in Algorithm 1. It allows K users to collaboratively fine-tune the auxiliary models with their local data and computation resources. A key advantage of this method is eliminating the need to iterate multiple adapters and save the computation space of auxiliary parameters and hidden representations in the forward pass and their corresponding gradient in the backward pass, as depicted in Table 1. In fact, by utilizing parameter merging, our method consumes the same amount of memory for a given batch size, regardless of the size of auxiliary models and the number of users, because the computation related to auxiliary models has been completely offloaded to low-cost devices. To the best of our knowledge, despite being a widely used technique, no previous work has explicitly studied the requirements of parameter merging. For any layer m to be fine-tuned, one wishes that the fine-tuned auxiliary model $g_{w_m}(\cdot)$

can be merged back to the original model architecture to simplify computation. The following result shows that $g_{w_m}(\cdot)$ must be linear in the input.

Proposition 2 Consider a linear function $x \mapsto f_\theta(x) = \theta x$, where $\theta \in \Theta \subseteq \mathbb{R}^{d_1 \times d_2}$ is the parameter and $x \in \mathbb{R}^{d_2}$. Assume that $g : \mathbb{R}^{d_2} \mapsto \mathbb{R}^{d_1}$ is such a function that $x \mapsto f_\theta(x) + g(x)$ can be equivalently written as $x \mapsto f_{\hat{\theta}}(x)$ for some $\hat{\theta} \in \Theta$. Then, g must be a linear function of x and written as wx for some $w \in \mathbb{R}^{d_1 \times d_2}$.

Remark 1 In the result above, $f_\theta(\cdot)$ represents the function of a generic layer, and $g(\cdot)$ denotes the auxiliary model. The parameterization of $g(\cdot)$ is not necessarily through w , as it could be a smaller parameter that maps to w . An example is the low-rank approximation $w = w_1 \cdot w_2$ where w_1 has a small number of hidden sizes.

In Table 1, we compare the complexity of the computation space of FT, PEFT, and ColA. Existing PEFT methods require significantly less computational space compared to FT, primarily because the size of auxiliary parameters $w_{1:m,1:K}$ and their gradient $\nabla w_{1:M,1:K}$ is minimal. Nevertheless, PEFT methods still require the computation of $\nabla w_{1:M,1:K}$ together with $\nabla h_{1:M}$, $\nabla \tilde{h}_{1:M,1:K}$, because they utilize the classical gradient descent learning procedure. In contrast, our proposed method is *parameter-free* because it completely decouples the computation related to auxiliary parameters $\nabla w_{1:M,1:K}$ from the forward and backward pass of the base model. If the parameter merging technique was used, ColA (merged) only computes the gradient of hidden representations $\nabla h_{1:M}$ on GPU. As a result, ColA (merged) can even reduce the cost of full fine-tuning by offloading all other computations to low-cost devices. To our knowledge, this has not been achieved with any existing methods. It indicates that our method can achieve the performance of full parameter training from scratch while reducing the computation space bottleneck. As depicted in Table 1, PEFT methods would multiply the cost of computational space on the GPU by K , whereas ColA (merged) incurs no additional overhead on the GPU. Furthermore, our method can effectively leverage distributed low-cost devices to optimize the auxiliary models in parallel. Thus, our method emerges as a more cost-effective and scalable option for FTaaS compared with existing PEFT methods. While our approach introduces additional runtime due to the transmission of adaptation data and auxiliary models from one device to another, we consider this a technical limitation, which could potentially be mitigated with further engineering refinements. For example, we can instead offload the computation to low-end GPUs instead of CPUs to speed up the transmission.

Table 1: The complexity of computation space of FT, PEFT, and ColA. Representations, parameters and their gradient in $\{\cdot\}$ can be stored in low-cost devices. $h_{1:M,1:K}$ denotes hidden representations of the base model and $\tilde{h}_{1:M,1:K}$ denotes the hidden representations of the auxiliary models.

Method		Forward		Backward	
		Representations	Parameters	Representations	Parameters
FT	Inference	—	$\theta_{1:M}$	—	—
	Learning	$h_{1:M}$	$\theta_{1:M}$	$\nabla h_{1:M}$	$\nabla \theta_{1:M}$
PEFT	unmerged	Inference	$\theta_{1:M}, w_{1:M,1:K}$	—	—
	Learning	$h_{1:M}, \tilde{h}_{1:M,1:K}$	$\theta_{1:M}, w_{1:M,1:K}$	$\nabla h_{1:M}, \nabla \tilde{h}_{1:M,1:K}$	$\nabla w_{1:M,1:K}$
	merged	Inference	$\theta_{1:M}$	—	—
ColA	unmerged	Inference	$\theta_{1:M}, w_{1:M,1:K}$	—	—
	Learning	$h_{1:M}, \tilde{h}_{1:M,1:K}$	$\theta_{1:M}, w_{1:M,1:K}$	$\nabla h_{1:M}, \nabla \tilde{h}_{1:M,1:K}$	$\{\nabla w_{1:M,1:K}\}$
	merged	Inference	$\theta_{1:M}$	—	—
	Learning	$h_{1:M}, \{\tilde{h}_{1:M,1:K}\}$	$\theta_{1:M}, \{w_{1:M,1:K}\}$	$\nabla h_{1:M}, \{\nabla \tilde{h}_{1:M,1:K}\}$	$\{\nabla w_{1:M,1:K}\}$

Our method, rooted in a functional gradient descent learning framework, is notably *model-agnostic*. The choice of auxiliary models $g_{w_{1:M,1:K}}(\cdot)$ is independent of the base model $f_\theta(\cdot)$. Moreover, different model architectures can be utilized for auxiliary models at various layers. It is crucial to recognize that the architecture of these auxiliary models significantly influences performance. For example, rather than using low-rank approximations like LoRA, it is feasible to utilize a linear layer or even a Multi-Layer Perceptron (MLP), because the computation of these auxiliary models is decoupled from that of the base model and offloaded to other devices. Also, interactive auxiliary

models, such as those in ControlNet (Zhang & Agrawala, 2023), where one model’s output serves as another’s input, may also utilize the proposed method. As depicted in Figure 1, another advantage of our model-agnostic approach is that the users of FTaaS can locally fine-tune their adapters using adaptation data received from the server if they have computational resources. Additionally, based on their available computational resources, users have the flexibility to customize the optimization of their adapters.

4 EXPERIMENTAL STUDIES

4.1 EXPERIMENTAL SETUP

We compare CoLA with full fine-tuning (FT) and PEFT methods including LoRA (Hu et al., 2021), AdaLoRA (Zhang et al., 2023), IA3 (Liu et al., 2022), Prompt Tuning (Lester et al., 2021), Prefix Tuning (Li & Liang, 2021), and P-Tuning (Liu et al., 2023). We conduct experiments on three tasks including Sequence Classification (SC), Sequence to Sequence (S2S), and Causal Language Modeling (CLM). For the SC task, we use RoBERTa (base) (Liu et al., 2019) as the pretrained model with GLUE benchmark for all methods (Wang et al., 2018). In the S2S task, we use BART (base) (Lewis et al., 2019) as the pretrained model and evaluate all methods with a range of datasets including Financial Phrase Bank (FPB) (Malo et al., 2014), WikiSQL (Zhong et al., 2017), SAMSum (Gliwa et al., 2019), E2E NLG (Dušek et al., 2020), WebNLG (Gardent et al., 2017), and DART (Nan et al., 2020). For the CLM task, we utilize GPT-2 (Radford et al., 2019) and Llama-2 (Touvron et al., 2023) as the pretrained model with the Dolly (Conover et al., 2023) dataset to perform instruction tuning (Wei et al., 2021).

We conduct experiments using Low Rank, Linear, and Multi-Layer Perceptron (MLP) auxiliary models to demonstrate the model-agnostic nature of our proposed CoLA method. For the low-rank variant of CoLA, termed as CoLA (Low Rank), we use a hidden dimension $r = 8$, identical to those of LoRA and AdaLoRA to ensure a consistent evaluation across methods. Our Linear auxiliary model has parameters that match the count of the weight matrix it fine-tunes, while our MLP configuration uses a two-layer neural network with a hidden size of 128 and ReLU activation. We apply the default configurations from the PEFT package (Mangrulkar et al., 2022) for other PEFT baselines. We demonstrate the hyperparameters used in our experiments in Table 5. Further experimental results including learning from scratch, adaptation interval, computation evaluation, and learning curves are available in the Appendix.

4.2 EXPERIMENTAL RESULTS

We demonstrate the results of RoBERTa (base) on the SC task with GLUE metric in Table 2 and the results of BART (base) on the S2S task with ROUGE (Longest) metric in Table 3. Compared with the existing PEFT methods, CoLA consistently outperforms PEFT methods including IA3, Prompt Tuning, Prefix Tuning, and P-Tuning. Furthermore, CoLA outperforms AdaLoRA on average for both SC and S2S tasks with fewer trainable parameters. Meanwhile, CoLA performs on par with LoRA across most datasets.

Table 2: Results of RoBERTa (base) on the Sequence Classification task with GLUE metric. The gradient of parameters in $\{\cdot\}$ can be stored in low-cost devices. Both parameters and their gradient in $[\cdot]$ can be stored in low-cost devices.

Method	Trainable Parameters	MNLI	SST-2	MRPC	CoLA	QNLI	QQP	RTE	STS-B	Avg.	
FT	125.2 M (100.0 %)	87.2	95.0	89.3	61.8	93.0	91.8	76.0	90.4	85.6	
LoRA	887.0 K (0.7 %)	86.7	95.1	89.4	62.8	93.0	90.9	75.1	90.3	85.4	
AdaLoRA	11.3 M (9.0 %)	87.5	95.2	88.2	60.3	93.1	91.4	65.3	90.2	83.9	
IA3	629.0 K (0.5 %)	85.1	93.8	83.2	52.6	91.4	88.7	65.7	87.5	81.0	
Prompt Tuning	607.5 K (0.5 %)	79.2	93.0	75.7	16.2	86.8	82.9	57.9	62.6	69.3	
Prefix Tuning	960.8 K (0.8 %)	85.3	93.2	72.3	23.4	90.6	88.9	61.7	66.9	72.8	
P-Tuning	821.5 K (0.7 M %)	80.6	93.5	77.1	27.8	89.0	84.4	59.1	85.4	74.6	
CoLA (Low Rank)	unmerged	{887.0 K (0.7 %)}	86.9	94.6	90.4	61.1	93.2	90.9	73.6	90.2	85.1
	merged	[887.0 K (0.7 %)]	86.7	94.5	88.5	62.3	93.0	90.8	75.1	90.1	85.1
CoLA (Linear)	unmerged	{14.7 M (11.8 %)}	87.2	95.4	88.5	61.3	92.9	90.9	71.8	90.9	84.9
	merged	[14.7 M (11.8 %)]	87.1	95.4	88.7	59.4	92.9	90.9	72.2	91.0	84.7
CoLA (MLP)	unmerged	{8.5 M (6.7 %)}	86.9	95.1	90.4	64.6	92.4	91.3	73.6	90.7	85.6

It is worth noting that fine-tuning for SC requires training the classifier layers from scratch due to distinct target classes across datasets. While LoRA typically fine-tunes these classifier layers in

conjunction with the auxiliary models, Gradient Learning (GL) computes the gradient of hidden representations during the backward pass of the base model. Consequently, we use a ‘Linear’ auxiliary model to train the newly initialized classifier layers. The results in Table 2 and 3 demonstrate that CoLA (Low Rank) methods closely align with LoRA in performance, as the gradient computed with our methods exactly matches the gradient of LoRA. In our evaluations, we also compare different auxiliary models. The results demonstrate that the selection of an auxiliary model can influence the model performance, as CoLA (Linear) and CoLA (MLP) can outperform CoLA (Low Rank). Notably, our proposed method can fine-tune without low-rank approximation while not incurring any additional cost of computation space, because the computation has been offloaded to separate low-cost devices.

Table 3: Results of BART (base) on the Sequence to Sequence task with ROUGE (Longest) metric. The gradient of parameters in $\{\cdot\}$ can be stored in low-cost devices. Both parameters and their gradient in $[\cdot]$ can be stored in low-cost devices.

Method	Trainable Parameters	FPB	WikiSQL	SAMSum	E2E NLG	WebNLG	DART	Avg.	
FT	139.4 M (100.0 %)	95.6	94.8	39.6	51.0	63.5	54.8	66.6	
LoRA	442.4 K (0.3 %)	96.5	94.9	39.0	50.9	62.7	54.5	66.4	
AdaLoRA	13.0 M (9.3 %)	93.8	95.4	38.7	50.9	63.4	55.1	66.2	
IA3	36.9 K (0.03 %)	71.4	86.0	34.6	49.7	53.9	49.9	57.6	
Prompt Tuning	30.7 K (0.02 %)	71.8	75.8	32.1	44.0	40.2	38.9	50.5	
Prefix Tuning	184.3 K (0.1 %)	75.8	83.6	27.7	33.6	33.9	33.1	47.9	
P-Tuning	244.7 K (0.2 %)	82.8	77.7	31.6	40.8	33.3	37.3	50.6	
CoLA (Low Rank)	unmerged	{442.4 K (0.3 %)}	95.6	94.8	38.9	50.9	62.4	54.7	66.2
	merged	[442.4 K (0.3 %)]	96.5	94.7	38.7	51.0	62.5	54.6	66.3
CoLA (Linear)	unmerged	{21.2 M (15.2 %)}	96.9	95.4	39.4	50.5	63.1	54.6	66.6
	merged	[21.2 M (15.2 %)]	98.2	95.6	39.0	50.8	63.1	55.0	66.9
CoLA (MLP)	unmerged	{11.8 M (8.5 %)}	98.2	95.5	39.9	51.0	63.5	54.7	67.1

We demonstrate the results of user collaboration in Table 4. In the ‘Joint’ setup, all data is jointly trained with the same set of auxiliary models. The ‘Alone’ setup trains each data subset without merging the auxiliary models. In contrast, the ‘Collaboration’ setup merges auxiliary parameters together. Notably, users have the flexibility to determine local model architecture. For instance, CoLA (Low Rank-Linear) indicates that the first four subsets (Classification, Information Extraction, Summarization, and Brainstorming) utilize CoLA (Low Rank), while the remaining subsets use CoLA (Linear). Results indicate that models trained in the ‘Collaboration’ setup perform on par with the ‘Joint’ and ‘Alone’ setup. However, the performance of ‘Alone’ diminishes after merging for inference, because ‘Alone’ setup does not utilize parameter merging during training.

Table 4: Results of GPT-2 on the Causal Language Modeling task with user collaboration. The gradient of parameters in $\{\cdot\}$ can be stored in low-cost devices. Both parameters and their gradient in $[\cdot]$ can be stored in low-cost devices.

Method		Trainable Parameters	Classification	Information Extraction	Summarization	Brainstorming	Creative Writing	Open Q&A	Closed Q&A	General Q&A	All		
											unmerged	merged	
Joint	Low Rank	unmerged	{294.9 K (0.2 %)}	19.9	12.4	16.5	13.2	14.5	14.9	15.0	16.6	15.5	15.5
		merged	[294.9 K (0.2 %)]	19.6	12.8	16.7	13.5	14.8	14.7	15.0	16.7	15.6	16.1
	Linear	unmerged	{21.2 M (17.1 %)}	21.8	13.3	17.2	14.0	14.1	15.5	15.3	16.3	16.1	16.1
		merged	[21.2 M (17.1 %)]	22.6	13.4	17.0	14.9	13.9	15.5	15.4	16.6	16.4	—
MLP	unmerged	{8.7 M (7.0 %)}	21.8	13.3	17.2	14.0	14.1	15.5	15.3	16.3	15.7	—	
Alone	Low Rank	$8 \times \{294.9 \text{ K}\}$	19.1	13.5	15.3	13.6	14.6	15.2	16.1	16.2	15.7	13.9	
	Low Rank-Linear	$4 \times \{294.9 \text{ K}\}, 4 \times \{21.2 \text{ M}\}$	18.9	11.2	15.7	13.7	13.7	15.5	16.3	16.2	15.5	13.9	
	Low Rank-MLP	$4 \times \{294.9 \text{ K}\}, 4 \times \{8.7 \text{ M}\}$	21.4	11.8	15.5	13.4	14.0	15.3	16.9	16.4	15.9	—	
Collaboration	Low Rank	$8 \times [294.9 \text{ K}]$	18.5	12.8	16.2	13.5	14.2	14.9	14.4	16.3	15.2	—	
	Low Rank-Linear	$4 \times [294.9 \text{ K}], 4 \times [21.2 \text{ M}]$	17.7	13.0	16.6	13.1	14.2	15.2	15.3	16.7	15.4	—	

We present ablation studies regarding the adaptation interval I in Section C.4. For these experiments, we use a batch size of $B = 8$. By increasing the adaptation interval, such as $I = 4$, the effective batch size becomes $B \times I$. The results indicate that it is possible to achieve satisfactory convergence with fewer updates to the auxiliary models. This extension becomes especially valuable in situations demanding extensive computational space for computing the gradient of hidden representations for numerous users of FTaaS.

5 CONCLUSION

In this work, we address the pressing challenge of efficiently fine-tuning pretrained models for downstream tasks without incurring prohibitive computational costs. As pretrained models continue to

grow in size and complexity, classical fine-tuning techniques have shown their limitations, especially when providing Fine-Tuning as a Service (FTaaS). We introduce Collaborative Adaptation (ColA) with Gradient Learning (GL), a parameter-free, model-agnostic fine-tuning approach that decouples the computation of the gradient of hidden representations and parameters and offloads the computation of the gradient to low-cost devices. We provide theoretical analysis and conduct extensive experiments to demonstrate that our method can perform on par or better than existing PEFT methods on various benchmarks with much less computation space bottleneck. Future works can further optimize the efficiency of the proposed method and broaden the application scope of FTaaS.

REFERENCES

- Tom Brown, Benjamin Mann, Nick Ryder, Melanie Subbiah, Jared D Kaplan, Prafulla Dhariwal, Arvind Neelakantan, Pranav Shyam, Girish Sastry, Amanda Askell, et al. Language models are few-shot learners. *Advances in neural information processing systems*, 33:1877–1901, 2020.
- Mike Conover, Matt Hayes, Ankit Mathur, Jianwei Xie, Jun Wan, Sam Shah, Ali Ghodsi, Patrick Wendell, Matei Zaharia, and Reynold Xin. Free dolly: Introducing the world’s first truly open instruction-tuned llm, 2023. URL <https://www.databricks.com/blog/2023/04/12/dolly-first-open-commercially-viable-instruction-tuned-llm>.
- Wenyuan Dai, Qiang Yang, Gui-Rong Xue, and Yong Yu. Boosting for transfer learning. In *Proceedings of the 24th international conference on Machine learning*, pp. 193–200, 2007.
- Tim Dettmers, Artidoro Pagnoni, Ari Holtzman, and Luke Zettlemoyer. Qlora: Efficient finetuning of quantized llms. *arXiv preprint arXiv:2305.14314*, 2023.
- Jacob Devlin, Ming-Wei Chang, Kenton Lee, and Kristina Toutanova. Bert: Pre-training of deep bidirectional transformers for language understanding. *arXiv preprint arXiv:1810.04805*, 2018.
- Enmao Diao, Jie Ding, and Vahid Tarokh. Heteroff: Computation and communication efficient federated learning for heterogeneous clients. *arXiv preprint arXiv:2010.01264*, 2020.
- Enmao Diao, Jie Ding, and Vahid Tarokh. Gal: Gradient assisted learning for decentralized multi-organization collaborations. *Advances in Neural Information Processing Systems*, 35:11854–11868, 2022.
- Enmao Diao, Ganghua Wang, Jiawei Zhan, Yuhong Yang, Jie Ding, and Vahid Tarokh. Pruning deep neural networks from a sparsity perspective. *arXiv preprint arXiv:2302.05601*, 2023.
- Ondřej Dušek, Jekaterina Novikova, and Verena Rieser. Evaluating the state-of-the-art of end-to-end natural language generation: The e2e nlg challenge. *Computer Speech & Language*, 59:123–156, 2020.
- William Fedus, Barret Zoph, and Noam Shazeer. Switch transformers: Scaling to trillion parameter models with simple and efficient sparsity. *The Journal of Machine Learning Research*, 23(1): 5232–5270, 2022.
- Yoav Freund and Robert E Schapire. A decision-theoretic generalization of on-line learning and an application to boosting. In *European conference on computational learning theory*, pp. 23–37. Springer, 1995.
- Jerome H Friedman. Greedy function approximation: a gradient boosting machine. *Annals of statistics*, pp. 1189–1232, 2001.
- Claire Gardent, Anastasia Shimorina, Shashi Narayan, and Laura Perez-Beltrachini. Creating training corpora for nlg micro-planning. In *55th annual meeting of the Association for Computational Linguistics (ACL)*, 2017.
- Bogdan Gliwa, Iwona Mochol, Maciej Biesek, and Aleksander Wawer. Samsun corpus: A human-annotated dialogue dataset for abstractive summarization. *arXiv preprint arXiv:1911.12237*, 2019.

-
- Junxian He, Chunting Zhou, Xuezhe Ma, Taylor Berg-Kirkpatrick, and Graham Neubig. Towards a unified view of parameter-efficient transfer learning. *arXiv preprint arXiv:2110.04366*, 2021.
- Neil Houlsby, Andrei Giurgiu, Stanislaw Jastrzebski, Bruna Morrone, Quentin De Laroussilhe, Andrea Gesmundo, Mona Attariyan, and Sylvain Gelly. Parameter-efficient transfer learning for nlp. In *International Conference on Machine Learning*, pp. 2790–2799. PMLR, 2019.
- Edward J Hu, Yelong Shen, Phillip Wallis, Zeyuan Allen-Zhu, Yanzhi Li, Shean Wang, Lu Wang, and Weizhu Chen. Lora: Low-rank adaptation of large language models. *arXiv preprint arXiv:2106.09685*, 2021.
- Furong Huang, Jordan Ash, John Langford, and Robert Schapire. Learning deep resnet blocks sequentially using boosting theory. In *International Conference on Machine Learning*, pp. 2058–2067. PMLR, 2018.
- Brian Lester, Rami Al-Rfou, and Noah Constant. The power of scale for parameter-efficient prompt tuning. *arXiv preprint arXiv:2104.08691*, 2021.
- Mike Lewis, Yinhan Liu, Naman Goyal, Marjan Ghazvininejad, Abdelrahman Mohamed, Omer Levy, Ves Stoyanov, and Luke Zettlemoyer. Bart: Denoising sequence-to-sequence pre-training for natural language generation, translation, and comprehension. *arXiv preprint arXiv:1910.13461*, 2019.
- Xiang Lisa Li and Percy Liang. Prefix-tuning: Optimizing continuous prompts for generation. *arXiv preprint arXiv:2101.00190*, 2021.
- Haokun Liu, Derek Tam, Mohammed Muqeeth, Jay Mohta, Tenghao Huang, Mohit Bansal, and Colin A Raffel. Few-shot parameter-efficient fine-tuning is better and cheaper than in-context learning. *Advances in Neural Information Processing Systems*, 35:1950–1965, 2022.
- Xiao Liu, Yanan Zheng, Zhengxiao Du, Ming Ding, Yujie Qian, Zhilin Yang, and Jie Tang. Gpt understands, too. *AI Open*, 2023.
- Yinhan Liu, Myle Ott, Naman Goyal, Jingfei Du, Mandar Joshi, Danqi Chen, Omer Levy, Mike Lewis, Luke Zettlemoyer, and Veselin Stoyanov. Roberta: A robustly optimized bert pretraining approach. *arXiv preprint arXiv:1907.11692*, 2019.
- Pekka Malo, Ankur Sinha, Pekka Korhonen, Jyrki Wallenius, and Pyry Takala. Good debt or bad debt: Detecting semantic orientations in economic texts. *Journal of the Association for Information Science and Technology*, 65(4):782–796, 2014.
- Sourab Mangrulkar, Sylvain Gugger, Lysandre Debut, Younes Belkada, and Sayak Paul. Peft: State-of-the-art parameter-efficient fine-tuning methods. <https://github.com/huggingface/peft>, 2022.
- Llew Mason, Jonathan Baxter, Peter Bartlett, and Marcus Frean. Boosting algorithms as gradient descent. *Advances in neural information processing systems*, 12, 1999.
- Niklas Muennighoff, Thomas Wang, Lintang Sutawika, Adam Roberts, Stella Biderman, Teven Le Scao, M Saiful Bari, Sheng Shen, Zheng-Xin Yong, Hailey Schoelkopf, et al. Crosslingual generalization through multitask finetuning. *arXiv preprint arXiv:2211.01786*, 2022.
- Linyong Nan, Dragomir Radev, Rui Zhang, Amrit Rau, Abhinand Sivaprasad, Chiachun Hsieh, Xiangru Tang, Aadit Vyas, Neha Verma, Pranav Krishna, et al. Dart: Open-domain structured data record to text generation. *arXiv preprint arXiv:2007.02871*, 2020.
- Atsushi Nitanda and Taiji Suzuki. Functional gradient boosting based on residual network perception. In *International Conference on Machine Learning*, pp. 3819–3828. PMLR, 2018.
- Adam Paszke et al. Pytorch: An imperative style, high-performance deep learning library. In *Advances in Neural Information Processing Systems 32*, pp. 8024–8035. Curran Associates, Inc., 2019.

-
- Matthew Peters, Mark E., Neumann, Mohit Iyyer, Matt Gardner, Christopher Clark, Kenton Lee, and Luke Zettlemoyer. Deep contextualized word representations. *Proceedings of the 2018 Conference of the North American Chapter of the Association for Computational Linguistics*, 2018.
- Alec Radford, Jeffrey Wu, Rewon Child, David Luan, Dario Amodei, Ilya Sutskever, et al. Language models are unsupervised multitask learners. *OpenAI blog*, 1(8):9, 2019.
- Sylvestre-Alvise Rebuffi, Hakan Bilen, and Andrea Vedaldi. Learning multiple visual domains with residual adapters. *Advances in neural information processing systems*, 30, 2017.
- Jie Ren, Samyam Rajbhandari, Reza Yazdani Aminabadi, Olatunji Ruwase, Shuangyan Yang, Minjia Zhang, Dong Li, and Yuxiong He. {ZeRO-Offload}: Democratizing {Billion-Scale} model training. In *2021 USENIX Annual Technical Conference (USENIX ATC 21)*, pp. 551–564, 2021.
- Robin Rombach, Andreas Blattmann, Dominik Lorenz, Patrick Esser, and Björn Ommer. High-resolution image synthesis with latent diffusion models. In *Proceedings of the IEEE/CVF conference on computer vision and pattern recognition*, pp. 10684–10695, 2022.
- Hugo Touvron, Thibaut Lavril, Gautier Izacard, Xavier Martinet, Marie-Anne Lachaux, Timothée Lacroix, Baptiste Rozière, Naman Goyal, Eric Hambro, Faisal Azhar, et al. Llama: Open and efficient foundation language models. *arXiv preprint arXiv:2302.13971*, 2023.
- Alex Wang, Amanpreet Singh, Julian Michael, Felix Hill, Omer Levy, and Samuel R Bowman. Glue: A multi-task benchmark and analysis platform for natural language understanding. *arXiv preprint arXiv:1804.07461*, 2018.
- Jason Wei, Maarten Bosma, Vincent Y Zhao, Kelvin Guu, Adams Wei Yu, Brian Lester, Nan Du, Andrew M Dai, and Quoc V Le. Finetuned language models are zero-shot learners. *arXiv preprint arXiv:2109.01652*, 2021.
- Elad Ben Zaken, Shauli Ravfogel, and Yoav Goldberg. Bitfit: Simple parameter-efficient fine-tuning for transformer-based masked language-models. *arXiv preprint arXiv:2106.10199*, 2021.
- Lvmin Zhang and Maneesh Agrawala. Adding conditional control to text-to-image diffusion models. *arXiv preprint arXiv:2302.05543*, 2023.
- Qingru Zhang, Minshuo Chen, Alexander Bukharin, Pengcheng He, Yu Cheng, Weizhu Chen, and Tuo Zhao. Adaptive budget allocation for parameter-efficient fine-tuning. *arXiv preprint arXiv:2303.10512*, 2023.
- Victor Zhong, Caiming Xiong, and Richard Socher. Seq2sql: Generating structured queries from natural language using reinforcement learning. *arXiv preprint arXiv:1709.00103*, 2017.

Appendix

A LIMITATION AND FUTURE WORKS

While our method decouples and offloads gradient computation, it requires the transfer of auxiliary model from the user to the server and adaptation data from the server to the user. This transfer saves computational space on the high-cost device hosting the large base model but introduces an additional run time due to data transmission. We consider this a technical limitation that could be addressed with engineering refinements, especially at the system level design of FTaaS.

Enhancing the computational efficiency of our method is another avenue for future work. Integrating strategies from efficient and distributed machine learning, such as quantization (Dettmers et al., 2023), pruning (Diao et al., 2023), and Federated Learning (Diao et al., 2020), may be beneficial. Another exciting direction for GL could involve more advanced gradient decoupling on the hidden representations (Huang et al., 2018), paving the way for extensive model parallelization to improve run-time efficiency. Moreover, integrating interactive auxiliary models with CoLA (Zhang & Agrawala, 2023) also represents a promising direction. Lastly, the applications of FTaaS could be further expanded by utilizing large language models (Touvron et al., 2023) and diffusion models (Rombach et al., 2022).

B THEORETICAL ANALYSIS

Proposition 1: The gradient $\nabla_{w_m} \ell_m(x, y; w_m)$ and $\nabla_{w_m} \mathcal{L}(y, f_\theta(x, \Delta h_{1:M}))$ evaluated at $w_m = w_m^t$ are the same for any w_m^t .

Proof 1 (Proof of Proposition 1) Suppose we evaluate the gradient of $\ell_m(x, y; w_m)$ and $\mathcal{L}(y, f_\theta(x, \Delta h_{1:M}))$ at w_m^t , which can be an arbitrary value at round t . By the definition of ℓ_m and the chain rule, we have

$$\frac{\partial \ell_m}{\partial w_m} = \frac{\partial \ell_m}{\partial g_{w_m}} \frac{\partial g_{w_m}}{\partial w_m} = (g_{w_m}(x_m) - (\Delta h_m - \nabla \hat{h}_m)) \frac{\partial g_{w_m}}{\partial w_m}. \quad (7)$$

Evaluating the above equality at w_m^t and using $\frac{\partial \hat{h}_m}{\partial g_{w_m}} \equiv 1$, we have

$$\left. \frac{\partial \ell_m}{\partial w_m} \right|_{w_m=w_m^t} = \nabla \hat{h}_m \frac{\partial g_{w_m}}{\partial w_m} = \frac{\partial \mathcal{L}}{\partial \hat{h}_m} \frac{\partial \hat{h}_m}{\partial g_{w_m}} \frac{\partial g_{w_m}}{\partial w_m} \Big|_{w_m=w_m^t} = \left. \frac{\partial \mathcal{L}}{\partial w_m} \right|_{w_m=w_m^t}, \quad (8)$$

where the last equality follows from the chain rule. This concludes the proof.

Proposition 2: Consider a linear function $x \mapsto f_\theta(x) = \theta x$, where $\theta \in \Theta \subseteq \mathbb{R}^{d_1 \times d_2}$ is the parameter and $x \in \mathbb{R}^{d_2}$. Assume that $g : \mathbb{R}^{d_2} \mapsto \mathbb{R}^{d_1}$ is such a function that $x \mapsto f_\theta(x) + g(x)$ can be equivalently written as $x \mapsto f_{\hat{\theta}}(x)$ for some $\hat{\theta} \in \Theta$. Then, g must be a linear function of x and written as wx for some $w \in \mathbb{R}^{d_2 \times d_1}$.

Proof 2 (Proof of Proposition 2) According to the assumption, there exists $\hat{\theta}$ such that

$$g(x) = f_{\hat{\theta}}(x) - f_\theta(x) = (\hat{\theta} - \theta)x, \quad (9)$$

so $g(x)$ can be written as wx with $w = \hat{\theta} - \theta$. This concludes the proof.

C EXPERIMENTAL STUDIES

C.1 EXPERIMENTAL SETUP

We demonstrate the hyperparameters used in the experiments in Table 5. We use a lower learning rate of 5.00E-6 for ColA (Linear) in some of the GLUE datasets, including MNLI, SST-2, QNLI, QQP, RTE, and Dolly dataset with Llama-2 base model, because the default learning rate is too large to converge. Due to computational constraints, we did not undertake extensive hyperparameter sweeps. Further tuning of hyperparameters might yield improved results. The auxiliary models of Llama-2 (Q , V) include query and value projection layers, while the auxiliary models of Llama-2 (All) include all projection layers.

Table 5: Hyperparameters used in the experiments.

Hyperparameter	FT	PEFT	ColA
Epoch		40	
Batch size		32	
Optimizer		AdamW	
Weight decay		5.00E-04	
Learning rate	5.00E-06	3.00E-04	
Scheduler		Linear decay	
Warm up		0.05	
Max sequence length		128	

C.2 EXPERIMENTAL RESULTS

The results for GPT-2 and Llama-2 (Q , V) on the CLM task evaluated using the ROUGE (Longest) metric are presented in Table 6 and 7. ColA (Low Rank) demonstrates performance comparable to LoRA with the same number of trainable parameters. Notably, ColA (Linear), despite its larger parameter count, outperforms both FT and LoRA. The sub-optimal performance of FT may be due to a low learning rate, which results in inadequate convergence. Notably, full Fine-Tuning (FT) does not fit in our 48 GB GPU as shown in Table 7.

Table 6: Results of GPT-2 on the Causal Language Modeling (CLM) task with ROUGE (Longest) metric. The gradient of parameters in $\{\cdot\}$ can be stored in low-cost devices. Both parameters and their gradient in $[\cdot]$ can be stored in low-cost devices.

Method	Trainable Parameters	Dolly
FT	124.4 M (100.0 %)	15.6
LoRA	294.9 K (0.2 %)	15.6
AdaLoRA	2.4 M (1.9 %)	14.2
IA3	36.9 K (0.03 %)	14.2
Prompt Tuning	15.4 K (0.01 %)	14.0
Prefix Tuning	368.6 K (0.3 %)	14.5
P-Tuning	229.4 K (0.2 %)	14.6
ColA (Low Rank)	unmerged {294.9 K (0.2 %)}	15.5
	merged [294.9 K (0.2 %)]	15.6
ColA (Linear)	unmerged {21.2 M (17.1 %)}	16.1
	merged [21.2 M (17.1 %)]	16.4
ColA (MLP)	unmerged {8.7 M (7.0 %)}	15.7

Table 7: Results of Llama-2 (Q, V) on the Causal Language Modeling (CLM) task with user collaboration. The gradient of parameters in $\{\cdot\}$ can be stored in low-cost devices. Both parameters and their gradient in $[\cdot]$ can be stored in low-cost devices.

Method		Trainable Parameters	Dolly
FT		6.7 B (100.0 %)	—
LoRA		4.2 M (0.06 %)	18.8
AdaLoRA		33.6 M (0.5 %)	18.9
IA3		393.2 K (0.006 %)	19.0
Prompt Tuning		81.9K (0.001 %)	18.8
Prefix Tuning		5.2 M (0.08 %)	16.3
P-Tuning		1.2 M (0.02 %)	18.0
CoLA (Low Rank)	unmerged	{4.2 M (0.06 %)}	19.3
	merged	[4.2 M (0.06 %)]	19.4
CoLA (Linear)	unmerged	{1.1 B (15.9 %)}	19.1
	merged	[1.1 B (15.9 %)]	19.0
CoLA (MLP)	unmerged	{103.0 M (1.5 %)}	19.2

Table 8: Results of Llama-2 (Q, V) on the Causal Language Modeling task with user collaboration. The gradient of parameters in $\{\cdot\}$ can be stored in low-cost devices. Both parameters and their gradient in $[\cdot]$ can be stored in low-cost devices.

Method		Trainable Parameters	Classification	Information Extraction	Summarization	Brainstorming	Creative Writing	Open Q&A	Closed Q&A	General Q&A	All	
Joint	Low Rank	unmerged {20.0 M (0.3 %)}	24.6	16.4	16.9	18.9	15.5	20.4	17.0	19.2	19.3	19.2
		merged [20.0 M (0.3 %)]	25.0	16.1	18.1	19.0	15.5	20.5	17.6	19.2	19.4	19.2
	Linear	unmerged {6.5 B (96.1 %)}	25.7	15.3	16.1	20.1	14.9	20.3	16.3	19.2	19.1	19.2
		merged [6.5 B (96.1 %)]	25.4	14.1	16.3	19.5	15.1	20.7	16.1	18.9	19.0	19.0
MLP	unmerged	{502.7 M (7.5 %)}	24.0	16.4	17.1	19.6	15.7	20.6	16.9	18.5	19.2	—
		[502.7 M (7.5 %)]	24.5	16.5	16.4	19.1	15.2	20.4	19.3	18.8	19.4	17.4
Alone	Low Rank	8 × {20.0 M}	23.2	14.2	17.2	19.0	14.3	20.5	19.2	19.4	19.2	—
	Low Rank-MLP	4 × {20.0 M}, 4 × {502.7 M}	23.8	14.7	16.0	19.5	15.8	20.4	16.2	19.0	18.8	—
Collaboration	Low Rank	8 × {20.0 M}	23.8	14.7	16.0	19.5	15.8	20.4	16.2	19.0	18.8	—

C.3 LEARNING FROM SCRATCH

Recall that CoLA (merged) can reduce the cost of full fine-tuning by offloading the computation of the gradient of parameters to other devices. It indicates that our method can achieve the performance of full parameter training from scratch while reducing the computation space bottleneck. To corroborate this, we trained the MNIST and CIFAR10 datasets on Linear, MLP, and CNN models from scratch. We train these models for 400 epochs with Stochastic Gradient Descent (SGD) and cosine annealing learning rate. The results demonstrate that LoRA yields suboptimal results due to low-rank approximation while our method can achieve the results of full-fine tuning because we can train the model without any approximation. Furthermore, MLP auxiliary models may also outperform full fine-tuning due to over-parameterization.

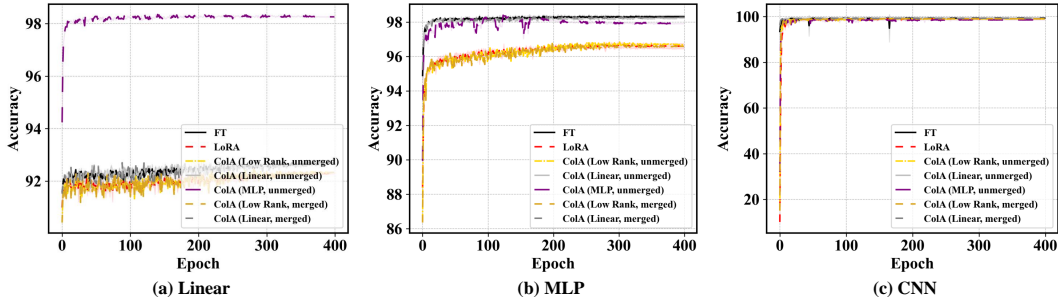


Figure 2: Learning curves of (a) Linear (b) MLP and (c) CNN with the MNIST dataset of IC task and Accuracy metric.

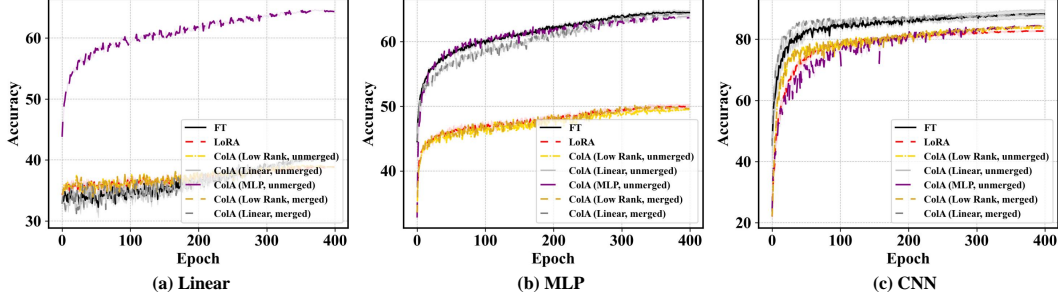


Figure 3: Learning curves of (a) Linear (b) MLP and (c) CNN with the CIFAR10 dataset of IC task and Accuracy metric.

Table 9: Results of learning Linear, MLP, and CNN from scratch on the Image Classification (IC) task with Accuracy metric. The gradient of parameters in $\{\cdot\}$ can be stored in low-cost devices. Both parameters and their gradient in $[\cdot]$ can be stored in low-cost devices.

Model	Method		Trainable Parameters	MNIST	CIFAR10
Linear	FT		7.9 K (100.0 %)	92.8	40.6
	LoRA		6.4k (80.9 %)	92.4	39.0
	CoLA (Low Rank)	unmerged	{6.4k (80.9 %)}	92.4	39.2
		merged	[6.4k (80.9 %)]	92.4	39.2
	CoLA (Linear)	unmerged	{7.9 K (100.0 %)}	92.7	40.7
		merged	[7.9 K (100.0 %)]	92.7	40.7
CoLA (MLP)	unmerged	{136.1K (1733.4 %)}	98.4	64.7	
MLP	FT		136.1 K (100.0 %)	98.4	64.7
	LoRA		12.5 K (9.2 %)	96.8	50.1
	CoLA (Low Rank)	unmerged	{12.5 K (9.2 %)}	96.8	49.6
		merged	[12.5 K (9.2 %)]	96.8	50.2
	CoLA (Linear)	unmerged	{136.1 K (100.0 %)}	98.3	64.1
		merged	[136.1 K (100.0 %)]	98.3	64.6
CoLA (MLP)	unmerged	{350.2 K (257.4 %)}	98.4	63.9	
CNN	FT		155.5 K (100.0 %)	99.4	88.3
	LoRA		44.2 K (2.8 %)	99.1	82.9
	CoLA (Low Rank)	unmerged	{44.2 K (2.8 %)}	99.2	84.0
		merged	[44.2 K (2.8 %)]	99.3	84.4
	CoLA (Linear)	unmerged	{155.5 K (100.0 %)}	99.4	88.3
		merged	[155.5 K (100.0 %)]	99.5	88.1
CoLA (MLP)	unmerged	{538.1 K (34.6 %)}	98.9	84.5	

C.4 ADAPTATION INTERVAL

We conduct ablation studies regarding the adaptation interval I . For these experiments, we use a batch size of $B = 8$ and CoLA (unmerged). By increasing the adaptation interval, such as $I = 4$, we can effectively increase the batch size from B to $B \times I$. In these experiments, we maintain the same number of training iterations T for different adaptation intervals. Therefore, experiments with $I = 8$ will update the auxiliary models at one-eighth the frequency of those experiments with $I = 1$. Furthermore, the results demonstrate that by tuning a proper adaptation interval, we can use less communication cost to achieve satisfactory performance. In particular, with a large effective batch size, we can estimate the gradient of parameters more accurately and potentially speed up the model convergence. This extension becomes especially valuable in situations demanding extensive computational space for computing the gradient of hidden representations for numerous users of FTaaS.

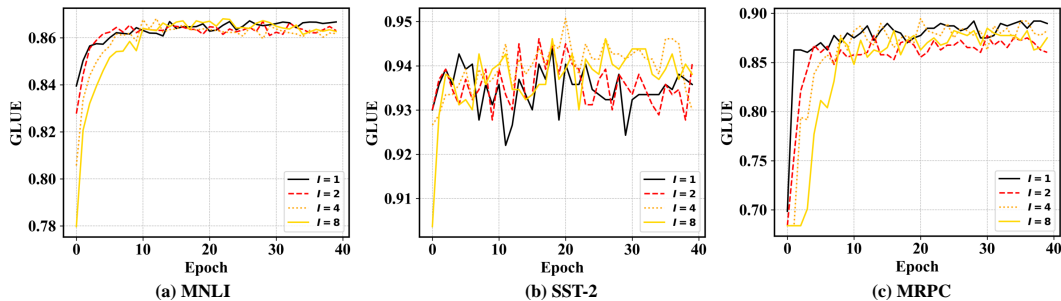


Figure 4: Ablation studies of adaptation interval I on (a) MNLI (b) SST-2, and (c) MRPC datasets of SC task and GLUE metric.

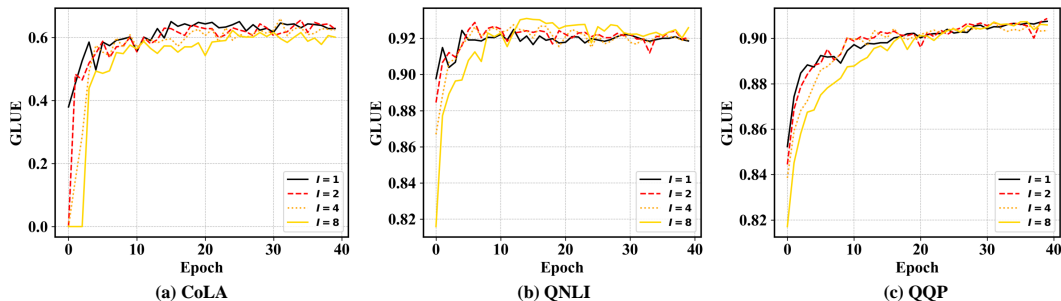


Figure 5: Ablation studies of adaptation interval I on (a) CoLA (b) QNLI, and (c) QQP datasets of SC task and GLUE metric.

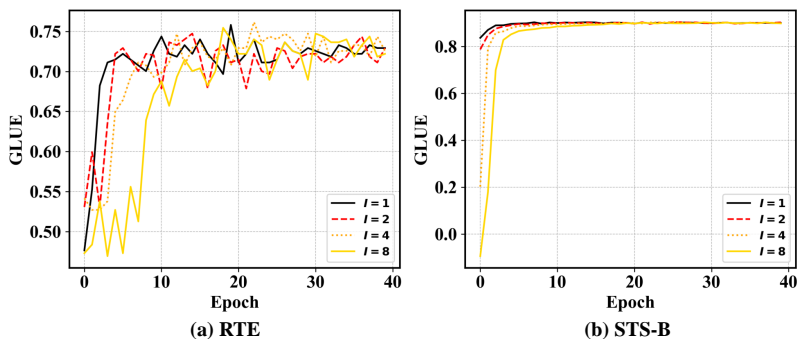


Figure 6: Ablation studies of adaptation interval I on (a) RTE and (b) STS-B datasets of SC task and GLUE metric.

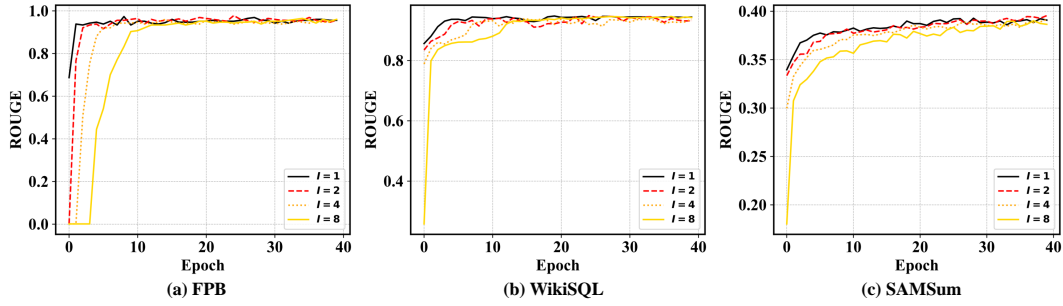


Figure 7: Ablation studies of adaptation interval I on (a) FPB (b) WikiSQL, and (c) SAMSum datasets of S2S task and ROUGE (Longest) metric.

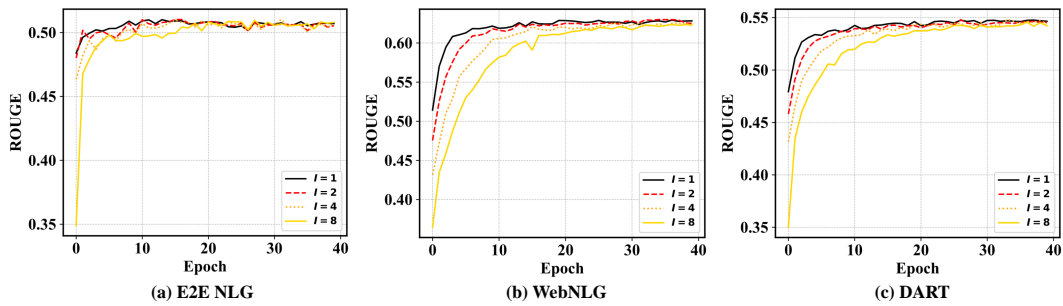


Figure 8: Ablation studies of adaptation interval I on (a) E2E NLG (b) WebNLG, and (c) DART datasets of S2S task and ROUGE (Longest) metric.

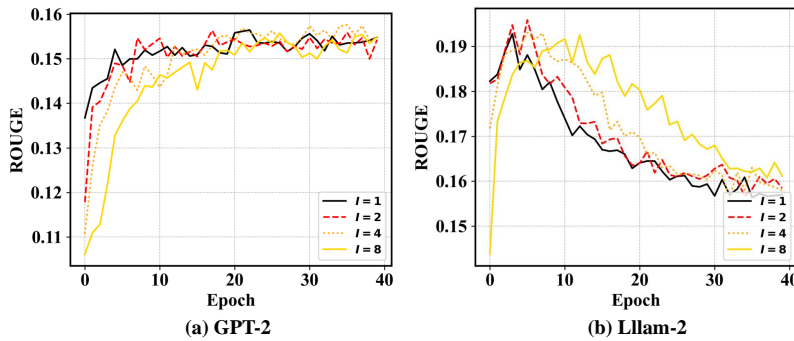


Figure 9: Ablation studies of adaptation interval I of (a) GPT-2 and (b) Llama-2 (Q, V) on Dolly dataset of CLM task and ROUGE (Longest) metric.

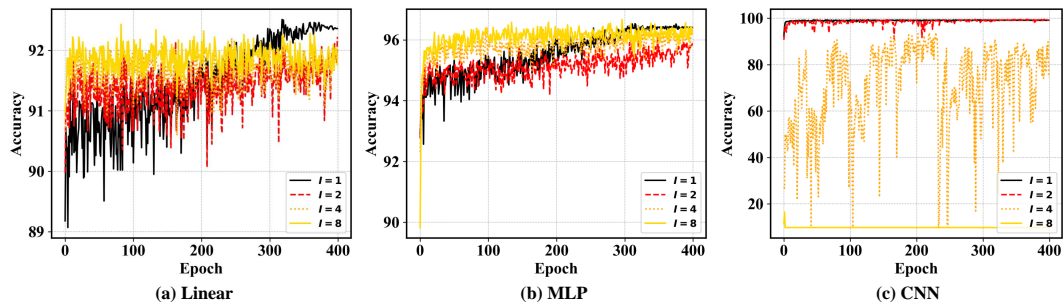


Figure 10: Ablation studies of adaptation interval I of (a) Linear, (b) MLP, and (c) CNN on MNIST dataset of IC task and Accuracy metric.

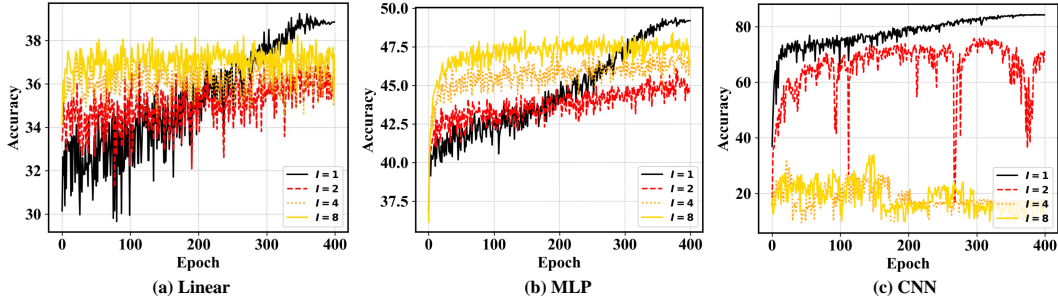


Figure 11: Ablation studies of adaptation interval I of (a) Linear, (b) MLP, and (c) CNN on CIFAR10 dataset of IC task and Accuracy metric.

C.5 COMPUTATION EVALUATION

We conduct a comprehensive quantitative evaluation of computational costs for all feasible experiments on real devices. We use an NVIDIA RTX A6000 (48 GB) as the primary host for the base model, with computation offloaded to a secondary device, either a CPU (Intel Xeon Gold 5320) with 944 GB RAM or another A6000. We carry out experiments by executing 10 training iterations with batch sizes of 1, 8, and 32, during which we measure computation space and run time.

The memory consumption of the primary device hosting the base model is noted as 'Memory (Base)'. To accurately evaluate the computation space for the gradient of auxiliary parameters, we measure the difference in memory consumption between two specific scenarios: one where computation is offloaded to a CPU, and another where it remains on the primary device. This difference in memory usage between these two cases is denoted as 'Memory (Offload)'. When the total memory usage exceeds 48 GB, we report the remaining memory on the primary GPU for 'Memory (Offload)'.

We also track the run time of the forward and backward pass of the base model, including the time taken to transfer adaptation data to another device, labeled as 'Offload to CPU (Base)' and 'Offload to GPU (Base)'. Additionally, we measure the run time for updating the auxiliary models on the secondary device, reporting the averaged run time across all adapters, as these models can be updated in parallel. In certain cases presented in Table 18, when the secondary A6000 GPU lacks the capacity to handle the offloaded memory, we do not report the run time.

The results, outlined in Tables 10 to 18, demonstrate a significant reduction in computation space bottleneck during the back-propagation of the base model through our method, while also indicating that run time can be decreased by offloading to an additional GPU. More specifically,

- Our method, CoLA (Low Rank), which matches LoRA exactly, consistently uses less computation space than LoRA during back-propagation of the base model.
- Despite the limited size of auxiliary models only providing a small advantage over LoRA (2-4 GB as shown in Table 13 and 14), our CoLA (Linear, merged) can train the network without low-rank approximation and significantly reduce the computation space bottleneck. For example, as shown in Table 13, CoLA (Linear, merged, batch size=8) requires 20.8 GB, compared to LoRA's 21.8 GB. Similarly, Table 14 shows that CoLA (Linear, merged, batch size=32) uses 42.8 GB, while LoRA exceeds 48 GB and does not fit on our device. Notably, our method also requires less computation space than direct training on the base model. For instance, full fine-tuning in Table 14 does not fit in 48 GB device even at a batch size of one.
- As demonstrated from Tables 16 to 18, CoLA (merged) consumes the same amount of memory for a given batch size, regardless of the size of auxiliary models and the number of users, because the computation of all auxiliary models has been completely offloaded to a separate device.
- The results demonstrate that the run time scales with batch size when we offload the computation to a CPU. However, offloading computation to an additional GPU significantly reduces run time. It is foreseeable as the communication of tensors among GPUs is much faster than it is between GPU and CPU. A pivotal aspect of our method is that the com-

putation of the gradient of model parameters can be *decoupled* from the classical back-propagation and *distributed* across multiple smaller devices with lower memory capacity. This is particularly desirable considering the affordability and availability of consumer-grade GPUs with smaller memory capacities, such as the 3090, in contrast to professional-grade GPUs like the H100.

Table 10: Computation evaluation of SC task with RoBERTa (base) model and GLUE (CoLA) dataset, where the number of auxiliary models $M = 26$.

Batch Size	Method	Trainable Parameters	Memory		Run Time (s)			
					Offload to CPU		Offload to GPU	
			Base	Offload	Base	Offload	Base	Offload
1	FT	125.2 M (100.0 %)	3.6 GB		0.037			
	LoRA	887.0 K (0.7 %)	1.1 GB		0.037			
	AdaLoRA	11.3 M (9.0 %)	1.3 GB		0.093			
	IA3	629.0 K (0.5 %)	1.1 GB		0.030			
	Prompt Tuning	607.5 K (0.5 %)	1.1 GB		0.029			
	Prefix Tuning	960.8 K (0.8 %)	1.1 GB		0.028			
	P-Tuning	821.5 K (0.7 M %)	1.1 GB		0.028			
	CoLA (Low Rank)	unmerged {887.0 K (0.7 %)}	1.1 GB	3.0 MB	0.091	0.002	0.034	0.001
		merged [887.0 K (0.7 %)]	1.1 GB	4.0 MB	0.081	0.002	0.066	0.001
	CoLA (Linear)	unmerged {14.7 M (11.8 %)}	1.2 GB	120.0 MB	0.055	0.003	0.035	0.001
		merged [14.7 M (11.8 %)]	1.1 GB	180.0 MB	0.071	0.002	0.073	0.001
CoLA (MLP)	unmerged {8.5 M (6.7 %)}	1.1 GB	60.0 MB	0.063	0.006	0.039	0.002	
8	FT	125.2 M (100.0 %)	3.6 GB		0.040			
	LoRA	887.0 K (0.7 %)	1.6 GB		0.043			
	AdaLoRA	11.3 M (9.0 %)	2.1 GB		0.108			
	IA3	629.0 K (0.5 %)	1.7 GB		0.032			
	Prompt Tuning	607.5 K (0.5 %)	1.8 GB		0.026			
	Prefix Tuning	960.8 K (0.8 %)	1.6 GB		0.034			
	P-Tuning	821.5 K (0.7 M %)	1.8 GB		0.026			
	CoLA (Low Rank)	unmerged {887.0 K (0.7 %)}	1.6 GB	12.8 MB	0.166	0.003	0.037	0.001
		merged [887.0 K (0.7 %)]	1.6 GB	5.2 MB	0.146	0.003	0.077	0.001
	CoLA (Linear)	unmerged {14.7 M (11.8 %)}	1.7 GB	130.8 MB	0.132	0.007	0.035	0.001
		merged [14.7 M (11.8 %)]	1.6 GB	212.0 MB	0.159	0.006	0.062	0.001
CoLA (MLP)	unmerged {8.5 M (6.7 %)}	1.7 GB	70.8 MB	0.157	0.009	0.041	0.002	
32	FT	125.2 M (100.0 %)	5.5 GB		0.093			
	LoRA	887.0 K (0.7 %)	3.3 GB		0.033			
	AdaLoRA	11.3 M (9.0 %)	4.4 GB		0.099			
	IA3	629.0 K (0.5 %)	3.7 GB		0.028			
	Prompt Tuning	607.5 K (0.5 %)	3.8 GB		0.021			
	Prefix Tuning	960.8 K (0.8 %)	3.4 GB		0.024			
	P-Tuning	821.5 K (0.7 M %)	3.8 GB		0.029			
	CoLA (Low Rank)	unmerged {887.0 K (0.7 %)}	3.2 GB	4.0 MB	0.273	0.005	0.052	0.003
		merged [887.0 K (0.7 %)]	3.2 GB	10.0 MB	0.264	0.004	0.081	0.004
	CoLA (Linear)	unmerged {14.7 M (11.8 %)}	3.3 GB	132.0 MB	0.300	0.012	0.047	0.003
		merged [14.7 M (11.8 %)]	3.2 GB	200.0 MB	0.281	0.009	0.078	0.004
CoLA (MLP)	unmerged {8.5 M (6.7 %)}	3.4 GB	62.0 MB	0.273	0.013	0.045	0.003	

Table 11: Computation evaluation of S2S task with BART (base) model and FPB dataset, where the number of auxiliary models $M = 36$

Batch Size	Method	Trainable Parameters	Memory		Run Time (s)				
			Base	Offload	Offload to CPU		Offload to GPU		
					Base	Offload	Base	Offload	
1	FT	139.4 M (100.0 %)	3.9 GB		0.054				
	LoRA	442.4 K (0.3 %)	1.1 GB		0.049				
	AdaLoRA	13.0 M (9.3 %)	1.4 GB		0.116				
	IA3	36.9 K (0.03 %)	1.2 GB		0.039				
	Prompt Tuning	30.7 K (0.02 %)	1.1 GB		0.028				
	Prefix Tuning	184.3 K (0.1 %)	1.1 GB		0.028				
	P-Tuning	244.7 K (0.2 %)	1.1 GB		0.028				
	CoLA (Low Rank)	unmerged	{442.4 K (0.3 %)}	1.1 GB	2.0 MB	0.099	0.002	0.054	0.001
		merged	[442.4 K (0.3 %)]	1.1 GB	6.0 MB	0.095	0.001	0.053	0.001
	CoLA (Linear)	unmerged	{21.2 M (15.2 %)}	1.2 GB	180.0 MB	0.078	0.004	0.045	0.001
		merged	[21.2 M (15.2 %)]	1.1 GB	260.0 MB	0.137	0.003	0.078	0.001
	CoLA (MLP)	unmerged	{11.8 M (8.5 %)}	1.2 GB	90.0 MB	0.091	0.006	0.068	0.002
	8	FT	139.4 M (100.0 %)	3.9 GB		0.037			
LoRA		442.4 K (0.3 %)	1.5 GB		0.044				
AdaLoRA		13.0 M (9.3 %)	1.9 GB		0.120				
IA3		36.9 K (0.03 %)	1.5 GB		0.037				
Prompt Tuning		30.7 K (0.02 %)	1.5 GB		0.029				
Prefix Tuning		184.3 K (0.1 %)	1.2 GB		0.030				
P-Tuning		244.7 K (0.2 %)	1.5 GB		0.034				
CoLA (Low Rank)		unmerged	{442.4 K (0.3 %)}	1.4 GB	4.0 MB	0.155	0.003	0.058	0.001
		merged	[442.4 K (0.3 %)]	1.4 GB	6.0 MB	0.118	0.002	0.061	0.001
CoLA (Linear)		unmerged	{21.2 M (15.2 %)}	1.6 GB	184.0 MB	0.142	0.005	0.047	0.001
		merged	[21.2 M (15.2 %)]	1.4 GB	304.0 MB	0.132	0.004	0.092	0.001
CoLA (MLP)		unmerged	{11.8 M (8.5 %)}	1.5 GB	90.0 MB	0.152	0.007	0.057	0.002
32		FT	139.4 M (100.0 %)	4.5 GB		0.069			
	LoRA	442.4 K (0.3 %)	2.6 GB		0.055				
	AdaLoRA	13.0 M (9.3 %)	3.3 GB		0.129				
	IA3	36.9 K (0.03 %)	2.8 GB		0.034				
	Prompt Tuning	30.7 K (0.02 %)	2.8 GB		0.033				
	Prefix Tuning	184.3 K (0.1 %)	1.5 GB		0.024				
	P-Tuning	244.7 K (0.2 %)	2.8 GB		0.029				
	CoLA (Low Rank)	unmerged	{442.4 K (0.3 %)}	2.5 GB	4.0 MB	0.255	0.003	0.059	0.001
		merged	[442.4 K (0.3 %)]	2.5 GB	6.0 MB	0.256	0.003	0.066	0.001
	CoLA (Linear)	unmerged	{21.2 M (15.2 %)}	2.6 GB	184.0 MB	0.258	0.007	0.051	0.001
		merged	[21.2 M (15.2 %)]	2.5 GB	272.0 MB	0.271	0.007	0.092	0.002
	CoLA (MLP)	unmerged	{11.8 M (8.5 %)}	2.6 GB	90.0 MB	0.234	0.009	0.065	0.002

Table 12: Computation evaluation of CLM task with GPT-2 model and Dolly dataset, where the number of auxiliary models $M = 12$

Batch Size	Method	Trainable Parameters	Memory		Run Time (s)				
			Base	Offload	Offload to CPU		Offload to GPU		
					Base	Offload	Base	Offload	
1	FT	124.4 M (100.0 %)	3.6 GB		0.031				
	LoRA	294.9 K (0.2 %)	1.3 GB		0.027				
	AdaLoRA	2.4 M (1.9 %)	1.3 GB		0.032				
	IA3	36.9 K (0.03 %)	1.3 GB		0.023				
	Prompt Tuning	15.4 K (0.01 %)	1.3 GB		0.021				
	Prefix Tuning	368.6 K (0.3 %)	1.3 GB		0.023				
	P-Tuning	229.4 K (0.2 %)	1.3 GB		0.028				
	CoLA (Low Rank)	unmerged	{294.9 K (0.2 %)}	1.3 GB	2.0 MB	0.063	0.002	0.033	0.001
		merged	[294.9 K (0.2 %)]	1.3 GB	4.0 MB	0.078	0.002	0.047	0.001
	CoLA (Linear)	unmerged	{21.2 M (17.1 %)}	1.3 GB	232.0 MB	0.066	0.005	0.034	0.001
		merged	[21.2 M (17.1 %)]	1.3 GB	312.0 MB	0.066	0.004	0.042	0.001
	CoLA (MLP)	unmerged	{8.7 M (7.0 %)}	1.3 GB	64.0 MB	0.080	0.007	0.035	0.002
	8	FT	124.4 M (100.0 %)	4.4 GB		0.029			
LoRA		294.9 K (0.2 %)	3.1 GB		0.027				
AdaLoRA		2.4 M (1.9 %)	3.2 GB		0.033				
IA3		36.9 K (0.03 %)	3.2 GB		0.027				
Prompt Tuning		15.4 K (0.01 %)	3.4 GB		0.025				
Prefix Tuning		368.6 K (0.3 %)	3.0 GB		0.024				
P-Tuning		229.4 K (0.2 %)	3.4 GB		0.026				
CoLA (Low Rank)		unmerged	{294.9 K (0.2 %)}	3.1 GB	2.0 MB	0.131	0.003	0.043	0.001
		merged	[294.9 K (0.2 %)]	3.1 GB	2.0 MB	0.140	0.004	0.052	0.001
CoLA (Linear)		unmerged	{21.2 M (17.1 %)}	3.2 GB	196.0 MB	0.158	0.012	0.035	0.001
		merged	[21.2 M (17.1 %)]	3.1 GB	276.0 MB	0.174	0.010	0.062	0.001
CoLA (MLP)		unmerged	{8.7 M (7.0 %)}	3.1 GB	12.0 MB	0.146	0.015	0.038	0.002
32		FT	124.4 M (100.0 %)	10.7 GB		0.150			
	LoRA	294.9 K (0.2 %)	9.2 GB		0.050				
	AdaLoRA	2.4 M (1.9 %)	9.2 GB		0.057				
	IA3	36.9 K (0.03 %)	9.6 GB		0.046				
	Prompt Tuning	15.4 K (0.01 %)	10.5 GB		0.055				
	Prefix Tuning	368.6 K (0.3 %)	8.8 GB		0.048				
	P-Tuning	229.4 K (0.2 %)	10.5 GB		0.056				
	CoLA (Low Rank)	unmerged	{294.9 K (0.2 %)}	9.0 GB	4.0 MB	0.998	0.015	0.080	0.007
		merged	[294.9 K (0.2 %)]	9.0 GB	16.0 MB	0.955	0.025	0.083	0.009
	CoLA (Linear)	unmerged	{21.2 M (17.1 %)}	9.1 GB	0B	1.012	0.027	0.089	0.007
		merged	[21.2 M (17.1 %)]	9.0 GB	92.0 MB	0.959	0.034	0.081	0.008
	CoLA (MLP)	unmerged	{8.7 M (7.0 %)}	9.1 GB	12.0 MB	1.026	0.032	0.092	0.008

Table 13: Computation evaluation of CLM task with Llama-2 (Q, V) model and Dolly dataset, where the number of auxiliary models $M = 64$. The auxiliary models of Llama-2 (Q, V) include query and value projection layers.

Batch Size	Method	Trainable Parameters	Memory		Run Time (s)				
					Offload to CPU		Offload to GPU		
			Base	Offload	Base	Offload	Base	Offload	
1	FT	6.7 B (100.0 %)	—		—				
	LoRA	4.2 M (0.06 %)	14.2 GB		0.105				
	AdaLoRA	33.6 M (0.5 %)	14.8 GB		0.146				
	IA3	393.2 K (0.006 %)	14.2 GB		0.107				
	Prompt Tuning	81.9K (0.001 %)	14.0 GB		0.082				
	Prefix Tuning	5.2 M (0.08 %)	14.1 GB		0.086				
	P-Tuning	1.2 M (0.02 %)	14.2 GB		0.084				
	CoLA (Low Rank)	unmerged	{4.2 M (0.06 %)}	14.0 GB	32.0 MB	0.274	0.003	0.135	0.001
		merged	[4.2 M (0.06 %)]	14.0 GB	120.0 MB	3.097	0.002	—	
	CoLA (Linear)	unmerged	{1.1 B (15.9 %)}	18.0 GB	8.2 GB	0.213	0.095	0.153	0.001
		merged	[1.1 B (15.9 %)]	14.0 GB	12.2 GB	2.675	0.040	—	
	CoLA (MLP)	unmerged	{103.0 M (1.5 %)}	14.4 GB	790.0 MB	0.248	0.007	0.157	0.002
	8	FT	6.7 B (100.0 %)	—		—			
		LoRA	4.2 M (0.06 %)	21.8 GB		0.197			
AdaLoRA		33.6 M (0.5 %)	22.4 GB		0.204				
IA3		393.2 K (0.006 %)	22.3 GB		0.190				
Prompt Tuning		81.9K (0.001 %)	22.3 GB		0.207				
Prefix Tuning		5.2 M (0.08 %)	21.0 GB		0.177				
P-Tuning		1.2 M (0.02 %)	22.3 GB		0.205				
CoLA (Low Rank)		unmerged	{4.2 M (0.06 %)}	20.6 GB	32.0 MB	0.607	0.004	0.277	0.002
		merged	[4.2 M (0.06 %)]	20.8 GB	68.0 MB	2.294	0.004	—	
CoLA (Linear)		unmerged	{1.1 B (15.9 %)}	24.6 GB	8.0 GB	0.683	0.113	0.360	0.005
		merged	[1.1 B (15.9 %)]	20.8 GB	12.0 GB	1.598	0.052	—	
CoLA (MLP)		unmerged	{103.0 M (1.5 %)}	21.3 GB	798.0 MB	0.640	0.015	0.279	0.002
32		FT	6.7 B (100.0 %)	—		—			
		LoRA	4.2 M (0.06 %)	46.6 GB		0.762			
	AdaLoRA	33.6 M (0.5 %)	47.3 GB		0.856				
	IA3	393.2 K (0.006 %)	—		—				
	Prompt Tuning	81.9K (0.001 %)	—		—				
	Prefix Tuning	5.2 M (0.08 %)	43.1 GB		0.686				
	P-Tuning	1.2 M (0.02 %)	—		—				
	CoLA (Low Rank)	unmerged	{4.2 M (0.06 %)}	42.7 GB	32.0 MB	8.893	0.063	—	
		merged	[4.2 M (0.06 %)]	42.7 GB	52.0 MB	8.069	0.081	—	
	CoLA (Linear)	unmerged	{1.1 B (15.9 %)}	46.7 GB	> 1.3 GB	9.260	0.244	—	
		merged	[1.1 B (15.9 %)]	42.7 GB	> 5.3 GB	7.392	0.233	—	
	CoLA (MLP)	unmerged	{103.0 M (1.5 %)}	43.4 GB	842.0 MB	8.789	0.075	—	

Table 14: Computation evaluation of CLM task with Llama-2 (All) model and Dolly dataset, where the number of auxiliary models $M = 228$. The auxiliary models of Llama-2 (All) include all projection layers.

Batch Size	Method	Trainable Parameters	Memory		Run Time (s)				
					Offload to CPU		Offload to GPU		
			Base	Offload	Base	Offload	Base	Offload	
1	FT	6.7 B (100.0 %)	—		—				
	LoRA	20.0 M (0.3 %)	15.0 GB		0.130				
	AdaLoRA	160.0 M (2.4 %)	17.7 GB		0.285				
	CoLA (Low Rank)	unmerged	{20.0 M (0.3 %)}	14.1 GB	160.0 MB	0.618	0.002	0.395	0.002
		merged	[20.0 M (0.3 %)]	14.1 GB	302.0 MB	14.938	0.002	—	—
	CoLA (Linear)	unmerged	{6.5 B (96.1 %)}	38.2 GB	> 9.8 GB	0.579	0.163	—	—
		merged	[6.5 B (96.1 %)]	14.1 GB	> 33.9 GB	13.311	0.064	—	—
	CoLA (MLP)	unmerged	{502.7 M (7.5 %)}	16.0 GB	4.0 GB	0.529	0.009	0.217	0.002
	8	FT	6.7 B (100.0 %)	—		—			
		LoRA	20.0 M (0.3 %)	25.6 GB		0.257			
AdaLoRA		160.0 M (2.4 %)	28.2 GB		0.359				
CoLA (Low Rank)		unmerged	{20.0 M (0.3 %)}	20.8 GB	160.0 MB	4.308	0.007	—	—
		merged	[20.0 M (0.3 %)]	20.9 GB	160.0 MB	13.768	0.008	—	—
CoLA (Linear)		unmerged	{6.5 B (96.1 %)}	44.9 GB	> 3.1 GB	4.708	0.189	—	—
		merged	[6.5 B (96.1 %)]	20.9 GB	> 27.1 GB	13.217	0.107	—	—
CoLA (MLP)		unmerged	{502.7 M (7.5 %)}	23.2 GB	3.9 GB	4.412	0.019	0.847	0.003
32		FT	6.7 B (100.0 %)	—		—			
		LoRA	20.0 M (0.3 %)	—		—			
	AdaLoRA	160.0 M (2.4 %)	—		—				
	CoLA (Low Rank)	unmerged	{20.0 M (0.3 %)}	43.2 GB	160.0 MB	41.026	0.083	—	—
		merged	[20.0 M (0.3 %)]	42.8 GB	320.0 MB	38.714	0.103	—	—
	CoLA (Linear)	unmerged	{6.5 B (96.1 %)}	—	—	—	—	—	—
		merged	[6.5 B (96.1 %)]	42.8 GB	> 5.2 GB	36.571	0.352	—	—
	CoLA (MLP)	unmerged	{502.7 M (7.5 %)}	45.9 GB	> 2.1 GB	40.676	0.099	—	—

C.6 LEARNING CURVES

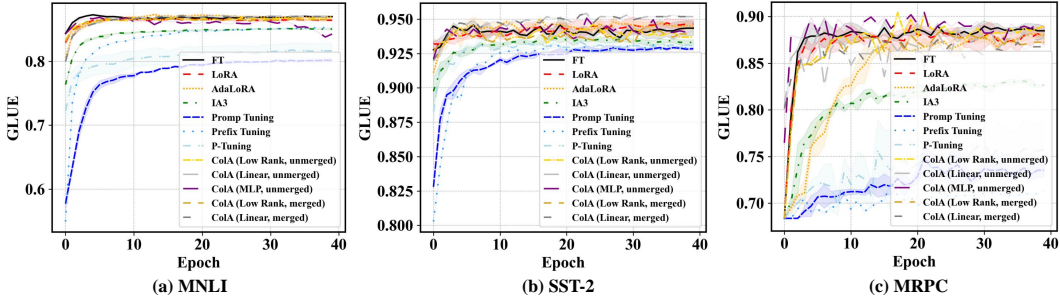


Figure 12: Learning curves of (a) MNLI (b) SST-2, and (c) MRPC datasets of SC task with and GLUE metric.

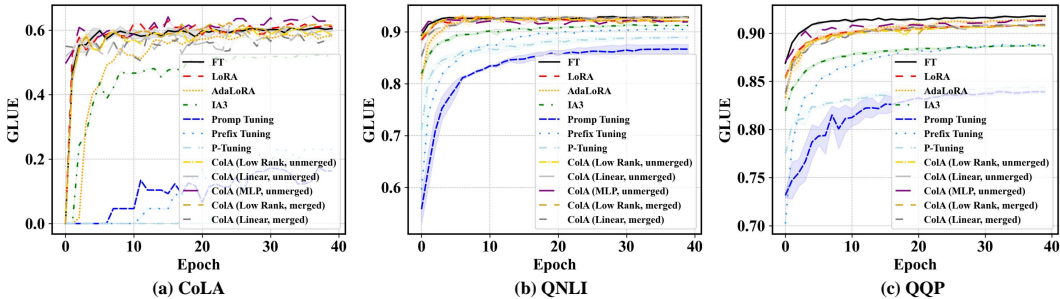


Figure 13: Learning curves of (a) CoLA (b) QNLI, and (c) QQP datasets of SC task and GLUE metric.

Table 15: Computation evaluation of IC task with Linear, MLP, CNN models and MNIST dataset.

Model	Batch Size	Method	Trainable Parameters	Memory		Run Time (s)				
				Base	Offload	Offload to CPU		Offload to GPU		
						Base	Offload	Base	Offload	
Linear, $M = 1$	1	FT		7.9 K (100.0 %)	545.8 MB			0.001		
		LoRA		6.4k (80.9 %)	545.8 MB			0.001		
		ColA (Low Rank)	unmerged	{6.4k (80.9 %)}	537.8 MB	8.0 MB	0.001	0.001	0.001	0.001
			merged	[6.4k (80.9 %)]	537.8 MB	8.0 MB	0.001	0.001	0.001	0.001
		ColA (Linear)	unmerged	{7.9 K (100.0 %)}	537.8 MB	8.0 MB	0.001	0.001	0.001	0.001
			merged	[7.9 K (100.0 %)]	537.8 MB	8.0 MB	0.002	0.001	0.001	0.001
	ColA (MLP)	unmerged	{136.1K (1733.4 %)}	537.8 MB	10.0 MB	0.001	0.002	0.001	0.002	
	8	FT		7.9 K (100.0 %)	545.8 MB			0.001		
		LoRA		6.4k (80.9 %)	545.8 MB			0.002		
		ColA (Low Rank)	unmerged	{6.4k (80.9 %)}	537.8 MB	8.0 MB	0.001	0.001	0.001	0.001
			merged	[6.4k (80.9 %)]	537.8 MB	8.0 MB	0.002	0.001	0.001	0.001
		ColA (Linear)	unmerged	{7.9 K (100.0 %)}	537.8 MB	8.0 MB	0.001	0.001	0.001	0.001
			merged	[7.9 K (100.0 %)]	537.8 MB	8.0 MB	0.001	0.001	0.001	0.001
	ColA (MLP)	unmerged	{136.1K (1733.4 %)}	537.8 MB	10.0 MB	0.001	0.002	0.001	0.002	
	32	FT		7.9 K (100.0 %)	545.8 MB			0.001		
LoRA		6.4k (80.9 %)	545.8 MB			0.001				
ColA (Low Rank)		unmerged	{6.4k (80.9 %)}	537.8 MB	8.0 MB	0.002	0.013	0.001	0.001	
		merged	[6.4k (80.9 %)]	537.8 MB	8.0 MB	0.001	0.001	0.002	0.002	
ColA (Linear)		unmerged	{7.9 K (100.0 %)}	537.8 MB	8.0 MB	0.001	0.001	0.001	0.001	
		merged	[7.9 K (100.0 %)]	537.8 MB	8.0 MB	0.001	0.001	0.002	0.001	
ColA (MLP)	unmerged	{136.1K (1733.4 %)}	537.8 MB	10.0 MB	0.001	0.002	0.001	0.002		
MLP, $M = 3$	1	FT		136.1 K (100.0 %)	547.8 MB			0.001		
		LoRA		12.5 K (9.2 %)	545.8 MB			0.001		
		ColA (Low Rank)	unmerged	{12.5 K (9.2 %)}	545.8 MB	0B	0.001	0.001	0.002	0.001
			merged	[12.5 K (9.2 %)]	545.8 MB	0B	0.003	0.001	0.003	0.002
		ColA (Linear)	unmerged	{136.1 K (100.0 %)}	547.8 MB	0B	0.002	0.001	0.003	0.001
			merged	[136.1 K (100.0 %)]	545.8 MB	2.0 MB	0.002	0.001	0.002	0.001
	ColA (MLP)	unmerged	{350.2 K (257.4 %)}	547.8 MB	2.0 MB	0.002	0.002	0.003	0.002	
	8	FT		136.1 K (100.0 %)	547.8 MB			0.001		
		LoRA		12.5 K (9.2 %)	545.8 MB			0.002		
		ColA (Low Rank)	unmerged	{12.5 K (9.2 %)}	545.8 MB	0B	0.002	0.001	0.002	0.001
			merged	[12.5 K (9.2 %)]	545.8 MB	0B	0.002	0.001	0.003	0.001
		ColA (Linear)	unmerged	{136.1 K (100.0 %)}	547.8 MB	0B	0.002	0.001	0.002	0.002
			merged	[136.1 K (100.0 %)]	545.8 MB	2.0 MB	0.002	0.001	0.003	0.002
	ColA (MLP)	unmerged	{350.2 K (257.4 %)}	547.8 MB	2.0 MB	0.002	0.002	0.003	0.003	
	32	FT		136.1 K (100.0 %)	547.8 MB			0.001		
LoRA		12.5 K (9.2 %)	545.8 MB			0.002				
ColA (Low Rank)		unmerged	{12.5 K (9.2 %)}	545.8 MB	0B	0.002	0.001	0.002	0.001	
		merged	[12.5 K (9.2 %)]	545.8 MB	0B	0.002	0.001	0.003	0.002	
ColA (Linear)		unmerged	{136.1 K (100.0 %)}	547.8 MB	0B	0.002	0.001	0.002	0.001	
		merged	[136.1 K (100.0 %)]	545.8 MB	2.0 MB	0.002	0.001	0.003	0.001	
ColA (MLP)	unmerged	{350.2 K (257.4 %)}	547.8 MB	2.0 MB	0.003	0.002	0.004	0.003		
CNN, $M = 5$	1	FT		155.5 K (100.0 %)	593.8 MB			0.003		
		LoRA		44.2 K (2.8 %)	721.8 MB			0.006		
		ColA (Low Rank)	unmerged	{44.2 K (2.8 %)}	719.8 MB	2.0 MB	0.009	0.002	0.005	0.002
			merged	[44.2 K (2.8 %)]	591.8 MB	132.0 MB	0.011	0.002	0.005	0.004
		ColA (Linear)	unmerged	{155.5 K (100.0 %)}	591.8 MB	22.0 MB	0.007	0.003	0.005	0.002
			merged	[155.5 K (100.0 %)]	591.8 MB	22.0 MB	0.009	0.002	0.005	0.002
	ColA (MLP)	unmerged	{538.1 K (34.6 %)}	593.8 MB	4.0 MB	0.007	0.003	0.006	0.002	
	8	FT		155.5 K (100.0 %)	615.8 MB			0.004		
		LoRA		44.2 K (2.8 %)	859.8 MB			0.004		
		ColA (Low Rank)	unmerged	{44.2 K (2.8 %)}	725.8 MB	6.0 MB	0.008	0.026	0.005	0.002
			merged	[44.2 K (2.8 %)]	593.8 MB	138.0 MB	0.007	0.002	0.006	0.005
		ColA (Linear)	unmerged	{155.5 K (100.0 %)}	613.8 MB	2.0 MB	0.013	0.004	0.005	0.002
			merged	[155.5 K (100.0 %)]	593.8 MB	22.0 MB	0.021	0.003	0.006	0.002
	ColA (MLP)	unmerged	{538.1 K (34.6 %)}	617.8 MB	2.0 MB	0.016	0.007	0.007	0.003	
	32	FT		155.5 K (100.0 %)	615.8 MB			0.003		
LoRA		44.2 K (2.8 %)	881.8 MB			0.005				
ColA (Low Rank)		unmerged	{44.2 K (2.8 %)}	765.8 MB	4.0 MB	0.035	0.022	0.005	0.002	
		merged	[44.2 K (2.8 %)]	633.8 MB	266.0 MB	0.022	0.006	0.005	0.004	
ColA (Linear)		unmerged	{155.5 K (100.0 %)}	633.8 MB	22.0 MB	0.019	0.005	0.006	0.002	
		merged	[155.5 K (100.0 %)]	633.8 MB	2.0 MB	0.020	0.005	0.006	0.002	
ColA (MLP)	unmerged	{538.1 K (34.6 %)}	695.8 MB	80.0 MB	0.012	0.017	0.007	0.002		

Table 16: Computation evaluation of CLM task with user collaboration, GPT-2 model, and Dolly dataset, where the number of auxiliary models $M = 12$ and the number of users $K = 8$.

Batch Size	Method	Trainable Parameters	Memory		Run Time (s)				
					Offload to CPU		Offload to GPU		
			Base	Offload	Base	Offload	Base	Offload	
1	Low Rank	unmerged	$8 \times \{294.9 \text{ K}\}$	1.3 GB	10.0 MB	0.073	0.004	0.040	0.004
		merged	$8 \times [294.9 \text{ K}]$	1.3 GB	70.0 MB	0.075	0.003	0.050	0.007
	Low Rank-Linear	unmerged	$4 \times \{294.9 \text{ K}\}, 4 \times \{21.2 \text{ M}\}$	1.6 GB	722.0 MB	0.061	0.017	0.035	0.002
		merged	$4 \times [294.9 \text{ K}], 4 \times [21.2 \text{ M}]$	1.3 GB	1.1 GB	0.064	0.004	0.053	0.006
	Low Rank-MLP	unmerged	$4 \times \{294.9 \text{ K}\}, 4 \times \{8.7 \text{ M}\}$	1.4 GB	196.0 MB	0.066	0.012	0.041	0.005
	8	Low Rank	unmerged	$8 \times \{294.9 \text{ K}\}$	3.1 GB	18.0 MB	0.190	0.013	0.075
merged			$8 \times [294.9 \text{ K}]$	3.1 GB	24.0 MB	0.095	0.010	0.051	0.019
Low Rank-Linear		unmerged	$4 \times \{294.9 \text{ K}\}, 4 \times \{21.2 \text{ M}\}$	3.6 GB	600.0 MB	0.135	0.031	0.065	0.019
		merged	$4 \times [294.9 \text{ K}], 4 \times [21.2 \text{ M}]$	3.1 GB	1.1 GB	0.129	0.020	0.050	0.023
Low Rank-MLP		unmerged	$4 \times \{294.9 \text{ K}\}, 4 \times \{8.7 \text{ M}\}$	3.2 GB	254.0 MB	0.178	0.024	0.080	0.024
32		Low Rank	unmerged	$8 \times \{294.9 \text{ K}\}$	9.0 GB	18.0 MB	1.000	0.017	0.205
	merged		$8 \times [294.9 \text{ K}]$	9.0 GB	40.0 MB	0.899	0.017	0.079	0.042
	Low Rank-Linear	unmerged	$4 \times \{294.9 \text{ K}\}, 4 \times \{21.2 \text{ M}\}$	9.4 GB	790.0 MB	1.059	0.034	0.186	0.038
		merged	$4 \times [294.9 \text{ K}], 4 \times [21.2 \text{ M}]$	9.0 GB	1.1 GB	0.971	0.030	0.075	0.017
	Low Rank-MLP	unmerged	$4 \times \{294.9 \text{ K}\}, 4 \times \{8.7 \text{ M}\}$	9.2 GB	58.0 MB	1.076	0.031	0.212	0.037

Table 17: Computation evaluation of CLM task with user collaboration, Llama-2 (Q, V), and Dolly dataset, where the number of auxiliary models $M = 64$ and the number of users $K = 8$. The auxiliary models of Llama-2 (Q, V) include query and value projection layers.

Batch Size	Method	Trainable Parameters	Memory		Run Time (s)				
					Offload to CPU		Offload to GPU		
			Base	Offload	Base	Offload	Base	Offload	
1	Low Rank	unmerged	$8 \times \{4.2 \text{ M}\}$	14.1 GB	128.0 MB	0.244	0.004	0.202	0.005
		merged	$8 \times [4.2 \text{ M}]$	14.0 GB	1.1 GB	1.655	0.003	—	—
	Low Rank-Linear	unmerged	$4 \times \{4.2 \text{ M}\}, 4 \times \{1.1 \text{ B}\}$	30.1 GB	> 7.9 GB	0.252	0.223	—	—
		merged	$4 \times [4.2 \text{ M}], 4 \times [1.1 \text{ B}]$	14.0 GB	> 34.0 GB	1.737	0.038	—	—
	Low Rank-MLP	unmerged	$4 \times \{4.2 \text{ M}\}, 4 \times \{103.0 \text{ M}\}$	15.6 GB	1.7 GB	0.216	0.011	0.356	0.005
	8	Low Rank	unmerged	$8 \times \{4.2 \text{ M}\}$	20.7 GB	256.0 MB	0.735	0.013	0.383
merged			$8 \times [4.2 \text{ M}]$	20.8 GB	828.0 MB	1.283	0.013	—	—
Low Rank-Linear		unmerged	$4 \times \{4.2 \text{ M}\}, 4 \times \{1.1 \text{ B}\}$	36.8 GB	> 11.2 GB	0.724	0.301	—	—
		merged	$4 \times [4.2 \text{ M}], 4 \times [1.1 \text{ B}]$	20.8 GB	> 27.2 GB	1.439	0.111	—	—
Low Rank-MLP		unmerged	$4 \times \{4.2 \text{ M}\}, 4 \times \{103.0 \text{ M}\}$	22.6 GB	3.1 GB	0.844	0.030	0.465	0.018
32		Low Rank	unmerged	$8 \times \{4.2 \text{ M}\}$	42.8 GB	256.0 MB	9.243	0.035	—
	merged		$8 \times [4.2 \text{ M}]$	42.7 GB	406.0 MB	6.316	0.030	—	—
	Low Rank-Linear	unmerged	$4 \times \{4.2 \text{ M}\}, 4 \times \{1.1 \text{ B}\}$	—	—	—	—	—	—
		merged	$4 \times [4.2 \text{ M}], 4 \times [1.1 \text{ B}]$	42.7 GB	> 5.3 GB	6.569	0.231	—	—
	Low Rank-MLP	unmerged	$4 \times \{4.2 \text{ M}\}, 4 \times \{103.0 \text{ M}\}$	44.6 GB	> 3.4 GB	9.216	0.065	—	—

Table 18: Computation evaluation of CLM task with user collaboration, Llama-2 (All), and Dolly dataset, where the number of auxiliary models $M = 224$ and the number of users $K = 8$. The auxiliary models of Llama-2 (All) include all projection layers.

Batch Size	Method	Trainable Parameters	Memory		Run Time (s)				
					Offload to CPU		Offload to GPU		
			Base	Offload	Base	Offload	Base	Offload	
1	Low Rank	unmerged	$8 \times \{20.0 \text{ M}\}$	14.6 GB	962.0 MB	0.627	0.004	0.305	0.002
		merged	$8 \times [20.0 \text{ M}]$	14.1 GB	4.5 GB	8.918	0.003	—	—
	Low Rank-Linear	unmerged	$4 \times \{20.0 \text{ M}\}, 4 \times \{6.5 \text{ B}\}$	—	—	—	—	—	—
		merged	$4 \times [20.0 \text{ M}], 4 \times [6.5 \text{ B}]$	14.1 GB	> 33.9 GB	8.959	0.051	0.356	0.003
	Low Rank-MLP	unmerged	$4 \times \{20.0 \text{ M}\}, 4 \times \{502.7 \text{ M}\}$	22.2 GB	11.7 GB	0.635	0.017	—	—
	8	Low Rank	unmerged	$8 \times \{20.0 \text{ M}\}$	21.6 GB	1.2 GB	4.583	0.015	1.133
merged			$8 \times [20.0 \text{ M}]$	20.9 GB	> 27.1 GB	7.956	0.016	—	—
Low Rank-Linear		unmerged	$4 \times \{20.0 \text{ M}\}, 4 \times \{6.5 \text{ B}\}$	—	—	—	—	—	—
		merged	$4 \times [20.0 \text{ M}], 4 \times [6.5 \text{ B}]$	20.9 GB	4.0 GB	6.949	0.171	—	—
Low Rank-MLP		unmerged	$4 \times \{20.0 \text{ M}\}, 4 \times \{502.7 \text{ M}\}$	29.7 GB	15.9 GB	5.588	0.044	1.311	0.008
32		Low Rank	unmerged	$8 \times \{20.0 \text{ M}\}$	44.2 GB	1.2 GB	41.893	0.058	—
	merged		$8 \times [20.0 \text{ M}]$	42.8 GB	3.5 GB	30.033	0.060	—	—
	Low Rank-Linear	unmerged	$4 \times \{20.0 \text{ M}\}, 4 \times \{6.5 \text{ B}\}$	—	—	—	—	—	—
		merged	$4 \times [20.0 \text{ M}], 4 \times [6.5 \text{ B}]$	42.8 GB	> 5.2 GB	30.818	0.440	—	—
	Low Rank-MLP	unmerged	$4 \times \{20.0 \text{ M}\}, 4 \times \{502.7 \text{ M}\}$	—	—	—	—	—	—

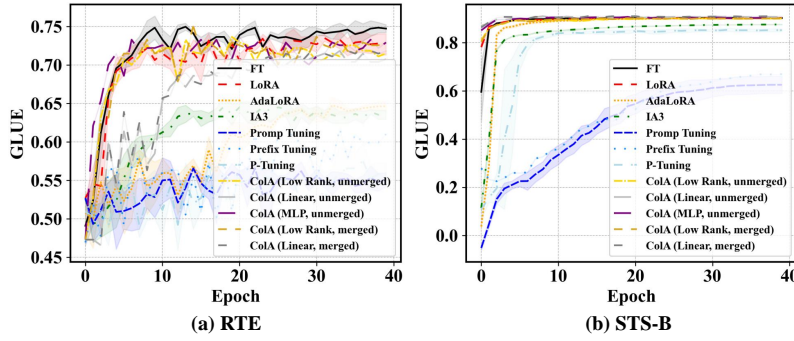


Figure 14: Learning curves of (a) RTE and (b) STS-B datasets of SC task and GLUE metric

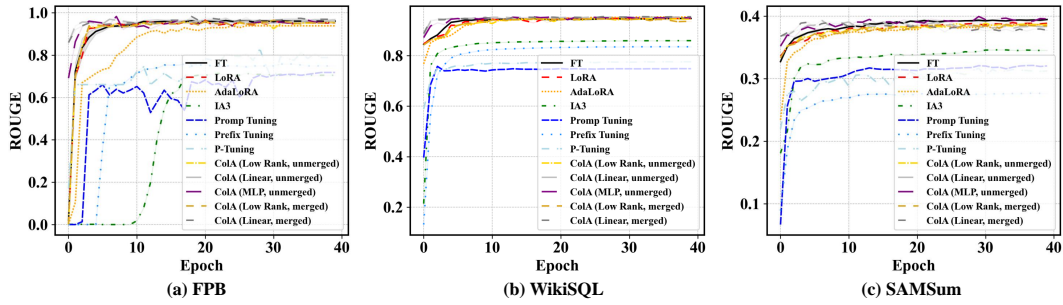


Figure 15: Learning curves of (a) FPB (b) WikiSQL, and (c) SAMSsum datasets of S2S task and ROUGE (Longest) metric.

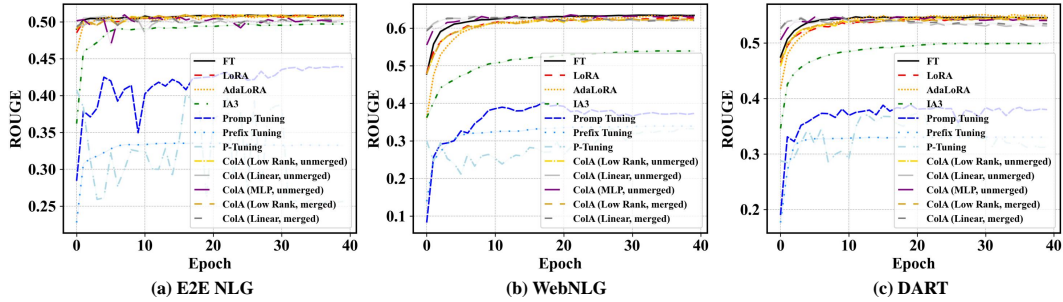


Figure 16: Learning curves of (a) E2E NLG (b) WebNLG, and (c) DART datasets of S2S task and ROUGE (Longest) metric.

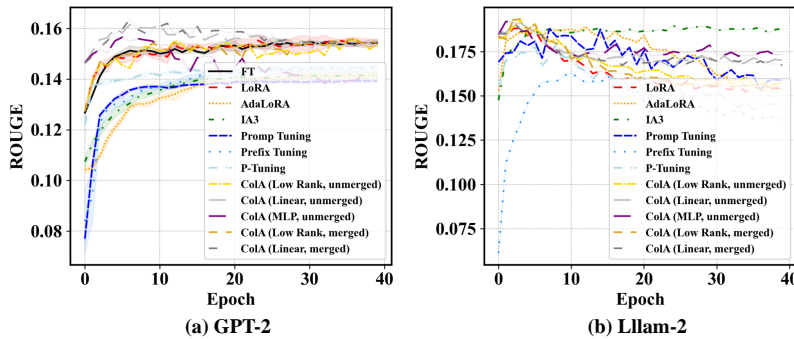


Figure 17: Learning curves of (a) GPT-2 and (b) Llama-2 (Q, V) on Dolly dataset of CLM task and ROUGE (Longest) metric.